PHASE TRANSITIONS IN MONOGLYCERIDE BILAYERS

A Light Scattering Study

G. E. CRAWFORD AND J. C. EARNSHAW
The Department of Pure and Applied Physics, The Queen's University of Belfast, Belfast BT7 1NN, Northern Ireland

ABSTRACT Thermotropic phase transitions in single planar bilayers of glycerol mono-oleate have been investigated using quasi-elastic light scattering from thermally excited membrane fluctuations. In certain cases both spectroscopic and intensity information were derived from the observations. For solvent-free bilayers transitional changes were observed in several membrane parameters: in tension, viscosity and thickness, in a combination of lipid orientational order parameter and dielectric anisotropy, and in the lateral compression modulus. These changes, particularly those in membrane thickness and in the anisotropy/order combination, were clearly indicative of a chain-melting transition in the lipid molecules. The chain-melting transition temperature was identified as 16.6 ± 0.03°C ($\Delta T_{1/2}$ = 1.5°C). The other changes tended to cluster around 12.5 and 16.6°C, suggesting that a two-stage transition was involved. Analysis of pretransitional fluctuations in membrane viscosity, based on a Landau approach, suggested that at the transition the membrane was close to a critical point (T^* = 12.7°C). Less information was accessible for membranes containing *n*-decane within their structure. In this case, the change in membrane tension was much smaller than in the solvent-free case and the transition was considerably broadened. These effects accord with an increase in 'interactive volume' within the bilayer due to solvent inclusion.

INTRODUCTION

Various biologically significant processes appear to be modulated by the thermotropic phase transitions that occur in the lipid component of biomembranes. Characterization of the transitions in pure lipid systems should provide a basis for understanding these biomembrane phenomena (1). Many different techniques (DSC, DTA, ESR, NMR, Raman, etc.) have been applied to a variety of model membrane systems. These studies have linked the main transition in such lipid systems to the cooperative *trans-gauche* isomerization about carbon–carbon bonds in the lipid hydrocarbon chains. In the high temperature, fluid 'liquid-crystalline' phase the lipid molecules, each possessing on average several *gauche* configurations, pack together in a relatively disordered state. In the low temperature, ordered 'gel' phase the lipid molecules, in all-*trans* configurations, can pack in a more ordered solid state.

Lipid membrane systems involve two-dimensionally ordered molecular arrangements. A two-dimensional solid may melt via a two-stage process, involving a novel intermediate phase (2). Among the two-dimensional systems that have been studied are liquid crystals; the smectic B-smectic A transition should be an exemplar of this two-stage melting. One model membrane system that may offer useful analogies is the planar lipid bilayer. Such bilayers are thin (thickness, $h \sim 4$ nm) and may appear effectively two-dimensional if $h \ll q^{-1}$, where q is the wave-number of those membrane motions probed by the experimental technique. This condition is necessary but may not be sufficient: the extra degrees of freedom inherent in the lipid hydrocarbon chains may override any strictly two-dimensional effects.

The various membrane systems used as models of biomembranes place different constraints upon the constituent lipid molecules, which may influence the phase transitions of the system. For example, in some model systems certain lipids have been found to display a lower or pretransition several degrees below the main chain-melting change. However, in unilamellar spherical vesicles the uniform tilt of the lipid molecules believed to occur between the lower and main transitions is forbidden and the lower transition is not observed (3). Again, a single planar lipid bilayer (hereafter BLM) lacks the interbilayer forces known to exist in multilamellar dispersions (e.g. 4) that may act to change the nature of the transition. Experimental work to date has concentrated upon multilamellar and vesicular systems, because most techniques would derive an inadequate signal from a single lipid bilayer. The dependence of the nature of the transition upon the membrane model used suggests that there is a place for experimental techniques capable of studying the transitions of single bilayers.

G. E. Crawford's present address is BKS Surveys Ltd., Ballycairn Road, Coleraine, Northern Ireland.

Laser light scattering from thermally excited fluctuations on planar lipid bilayers (see reference 5) is shown here to yield information about the membrane viscoelasticity, the membrane thickness, the dielectric anisotropy and orientational order parameters, and the in-plane membrane compressibility. Changes at bilayer phase transitions are observable in all these parameters. The light scattering method provides information on a single bilayer without introducing any molecular or other perturbation. The membrane properties measured are averages over the illuminated area of the BLM (radius ~ 300 μm). Some techniques applicable to single BLM involve insertion of probe molecules into the membrane (6) and provide information on the microscopic environment of the probe. Other methods involve macroscopic deformation of the BLM (e.g. 7). Light scattering methods illuminate molecular processes within the membrane without any perturbation of the system.

The experimental results presented here derive predominantly from studies of 'solvent-free' BLM of glycerol mono-oleate (GMO). Various thermally-induced changes in the properties of GMO bilayers, occurring over a range of temperatures about 15°C, have been reported (8, 9, 10, 11), but to date the exact nature of the transition involved has not been clearly established. No thermally detectable pretransition has been observed (8).

The next two sections of this paper present brief accounts of the relevant theoretical background and the experimental methods used. In view of detailed accounts in earlier publications (e.g. 5, 12), we concentrate here upon aspects that have not hitherto been significant or that are particularly relevant to studies of phase transitions. The following section presents data and their interpretation concerning first (and briefly) GMO bilayers containing appreciable quantities of solvent and second essentially solvent-free BLM. In the latter case a particularly detailed and unified picture of the transition emerges. The Discussion centers upon the nature of the transition in GMO bilayers and upon interconnections between the transitional changes in various membrane properties. Finally the Conclusions of this work are briefly summarized. The principal symbols used are identified in a Glossary for easy reference.

GLOSSARY

e_0	static lateral compression modulus of BLM
$\mathbf{f}$	polarization vector of scattered light
h	BLM thickness
$\mathbf{i}$	polarization vector in incident light
$\mathbf{n}$	orientation of lipid molecules in BLM
n_m	mean refractive index of BLM
n_0	refractive index of ambient medium
q	$2\pi/\Lambda$
q_z	component of scattering vector normal to BLM
A	amplitude of oscillatory correlation function
B	background to correlation function
C	BLM capacitance
ΔH_t	Enthalpy of BLM fusion
I	light intensity
I_c	I scattered by compression waves
I_r	I of heterodyne reference beam
I_s	measured I scattered by capillary waves
I_t	predicted I scattered by capillary waves
I_{tot}	total detected I
K	curvature elastic modulus
k_B	Boltzmann's constant
R	BLM reflectivity
S	BLM orientational order parameter
T_h	high temperature inflexion point of $S(T)$
T_t	main BLM transition temperature
T^*	critical temperature of BLM
γ_0	BLM tension
γ'	transverse shear viscosity of BLM
ϵ_0	dielectric constant of ambient fluid
ϵ_a	anisotropic dielectric constant of BLM
ϵ_m	mean dielectric constant of BLM
η	dynamic viscosity of ambient fluid
λ	wavelength of light
τ	relaxation time
ϕ	an order parameter of BLM
ω_0	capillary wave frequency
Γ	capillary wave temporal damping
Λ	capillary wavelength

THEORETICAL BACKGROUND

A lipid bilayer exhibits a variety of viscoelastic moduli that influence its motion. Several membrane vibrational modes arise, which may propagate or diffuse depending upon the balance of forces (driving and dissipative).

For a membrane comprising isotropic molecules up to five separate interfacial moduli may exist (13). One of these, slip of the membrane relative to the ambient fluids, can usually be neglected (14). The four remaining viscoelastic moduli can be separated into two pairs, each comprising a modulus describing compression (or dilation) and another describing shear. One pair acts in the membrane plane and the other normal to that plane (Fig. 1).

Each modulus can be expanded as a positive definite response function to explicitly demonstrate the elastic and viscous portions. The shear modulus transverse to the membrane is

$$\gamma = \gamma_0 - i\omega\gamma', \tag{1}$$

where γ_0 is identified as the usual static value of the interfacial tension (15). Some of the other moduli can similarly be identified with familiar membrane properties. The imaginary part of the in-plane shear modulus relates to the usual 'interfacial viscosity.' The real part of the in-plane dilational modulus is the conventional interfacial elastic modulus

$$e_0 = \partial\gamma_0/\partial \ln A \tag{2}$$

(e is here preferred to the more conventional ϵ to avoid subsequent confusion with dielectric constant). The viscoelastic response of a membrane cannot be summarized by *an* interfacial elasticity and *an* interfacial viscosity. The response discerned experimentally must depend upon the

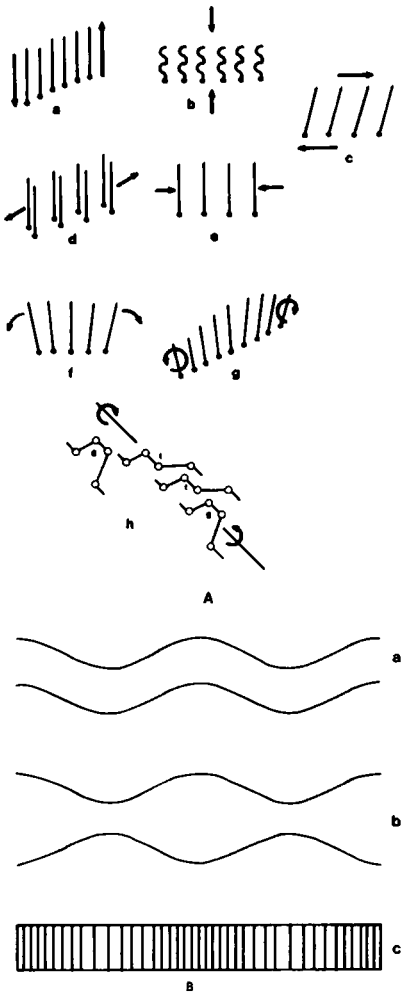

FIGURE 1 (*A*) The molecular motions possible in a lipid film (partly adapted from 13): (*a*) transverse shear; (*b*) transverse compression; (*c*) slip or horizontal shear; (*d*) lateral shear, (*e*) lateral compression; (*f*) splay in a molecular plane; (*g*) twist of a molecular plane; and (*h*) orientational order fluctations about molecular axes. (*B*) The three types of membrane fluctuation which scatter light: (*a*) transverse; (*b*) thickness; and (*c*) compression. *a* and *b* differ in the relative phases of the motion of the bilayer interfaces. In *a* the two interfaces move in sympathy whereas in *b* their motions are out of phase.

motions examined. Thus the interfacial viscosity determined in this work is γ', the transverse shear viscosity (Eq. 1).

The membrane modes associated with these four moduli are discussed below for the case of a membrane of optically isotropic molecules. Subsequently the more complicated case of a membrane comprising anisotropic molecules will briefly be examined. In both cases the membrane is assumed to be isotropic within its plane.

Membranes of Isotropic Molecules

Kramer (16) analyzes the fluctuations of an optically isotropic membrane, discussing three sets of modes (in-plane shear, transverse shear and in-plane compression). The fourth mode that would be expected—thickness fluctuations—can only be significant over a limited range of wave-lengths, set by the transverse compressibility of the membrane (17). For membranes formed from monoglycerides dispersed in squalene (similar to the present 'solvent-free' BLM) this compressibility is so low that q must exceed 10^6 cm^{-1} ($\Lambda < 10$ nm), far above the regime observed in our experiments (17).

The membrane displacement for each mode is assumed to behave as

$$\zeta(\mathbf{r}, t) = \zeta_0 \exp [i(\mathbf{q}.\mathbf{r} - \omega t)], \tag{3}$$

where q is the wave-number ($2\pi/\Lambda$) and ω is the complex frequency ($\omega = -i\Gamma \pm \omega_0$) of the fluctuation probed.

Leaving aside the thickness mode, two types of membrane fluctuation scatter light (Fig. 1). Kramer's mode involving in-plane shear couples to no other membrane motion and involves no perturbation of the dielectric constant. It will not be considered further. The remaining two membrane motions, the in-plane compression and transverse shear (or capillary) modes, are in general coupled. For the case of a symmetric bilayer (one separating identical fluids), the compression and transverse modes decouple (16). The dispersion equations for these modes are then

$$i\omega - \gamma q^3 (q - m)/2i\rho m\omega = 0 \tag{4}$$

for the transverse case and

$$i\omega - eq^2(q - m)/2i\rho\omega = 0 \tag{5}$$

for the compression modes. Here

$$m = [q^2 - i\omega\rho/\eta]^{1/2} \; Re(m) > 0. \tag{6}$$

In Eqs. 4 to 6 the density ρ and viscosity η refer to the ambient fluid and both γ and e are positive-definite response functions (cf Eq. 1). The elastic modulus e influences the transverse mode of a symmetric membrane only indirectly through changes in tension (Eq. 2).

Approximate solutions of these dispersion equations relate the mode frequency and wave-number more transparently to the properties of the system. For example, for the transverse waves

$$\omega_0^2 \simeq \gamma_0 q^3/2\rho \text{ and } \Gamma \simeq \eta q^2/\rho. \tag{7}$$

Higher order approximations, including the effect of γ', have been derived (5). The frequency of the compression waves is

$$\omega_0^3 \simeq e_0^2 q^4/4\eta\rho, \tag{8}$$

approximately.

Light incident upon the membrane will be scattered by the fluctuations in dielectric constant caused by these various membrane modes. The scattering process is illustrated in Fig. 2, where q is seen to be the component of the

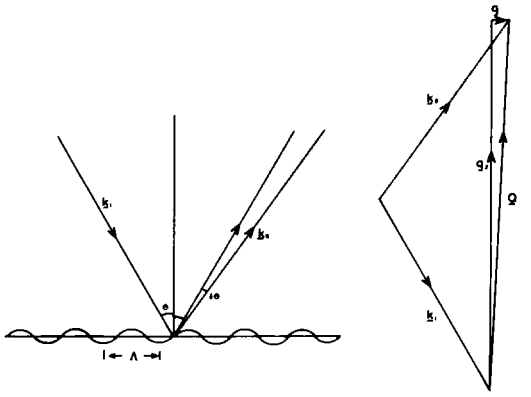

FIGURE 2 Scattering by an interfacial fluctuation of wave-vector q ($|q| = 2\pi/\Lambda$). Light incident with wave-vector $\mathbf{k}_i$ is scattered through a small angle $\delta\theta$ relative to the specular reflection, the scattered wave-vector is $\mathbf{k}_s$.

usual scattering vector ($\mathbf{Q} = \mathbf{k}_i - \mathbf{k}_s$) parallel to the membrane plane.

The spectrum of light scattered by thermally excited membrane fluctuations simply reflects the power spectrum of the fluctuations. The primary concern of the present paper is with transverse or capillary waves. In this case the spectrum of the scattered light is

$$P(\omega) = \frac{\tau^2 q}{2\rho}\frac{k_B T}{\pi\omega} Im\left\{\frac{(1+2S)^{1/2}-1}{D(S)}\right\}, \quad (9)$$

an approximately Lorentzian form with peak frequency ω_0 and linewidth Γ. In Eq. 9 the following abbreviations are used:

$$\tau = \frac{\rho}{2\eta q^2}, S = -i\omega\tau \quad (10)$$

and $D(S) = 0$ represents the dispersion equation (Eq. 4). These values of ω_0 and Γ are close to those given by the complex conjugate roots of the dispersion equation. While the capillary waves will be overdamped under certain conditions, the present experiments have all been in the propagating regime.

The intensity scattered by the various modes is given by Kramer as

$$\frac{1}{I_0}\frac{dI}{d\Omega} = \frac{\pi^2}{\lambda^4}\frac{k_B T}{Aq^2} \cdot \left\{\frac{(\epsilon_2-\epsilon_1)^2}{\gamma_0} + \frac{q_z^2 h^2 [\epsilon_m - \tfrac{1}{2}(\epsilon_1+\epsilon_2)]^2}{\gamma_0} + \frac{q^2h^2(\epsilon_m-1)^2}{e_0}\right\} \quad (11)$$

for incident light plane polarized perpendicular to the plane of incidence. In Eq. 11, A is the membrane area, h the membrane thickness and ϵ_1, ϵ_2, and ϵ_m the dielectric constants of the ambient fluids in the reflection and transmission half-spaces and the membrane respectively. The factor q_z is defined in Fig. 2. For a fluid surface, the scattering should be dominated by the first term of Eq. 11. Unfortunately the form of this term does not agree with other published results (18, 19): in particular the intensity scattered in the reflection half-space should include the surface reflectivity. Similar considerations will apply to the second term of Eq. 11, relating to scattering by capillary waves *upon* a membrane (20), but not to the final term, concerned with compression waves *within* the membrane (and hence fluctuations in ϵ_m alone). These arguments suggest that, for the case of a symmetric membrane ($\epsilon_2 = \epsilon_1 \equiv \epsilon_0$), Eq. 11 should be rewritten as

$$\frac{1}{I_0}\frac{dI}{d\Omega} = \frac{\pi^2}{\lambda^4}\frac{k_B T}{Aq^2} \cdot \left[\frac{q_z^2 h^2 R_{s,p}(\epsilon_m-\epsilon_0)^2}{\gamma_0} + \frac{q^2h^2(\epsilon_m-1)^2}{e_0}\right], \quad (12)$$

where $R_{s,p}$ is the reflectivity of an interface between media of ϵ_0 and ϵ_m for perpendicular (s) or parallel (p) polarization states of the incident light. The two terms of Eq. 12 will hereafter be referred to as I_t and I_c respectively (for the theoretically predicted intensities due to transverse and compression waves).

In general, e_0 considerably exceeds γ_0 for a bilayer and so I_c is much smaller than I_t. An experimental observation of the ratio of the two scattered intensities

$$\frac{I_t}{I_c} = \frac{e_0}{\gamma_0}\frac{q_z^2 R_{s,p}(\epsilon_m-\epsilon_0)^2}{q^2(\epsilon_m-1)^2} \quad (13)$$

would permit e_0 to be estimated relative to γ_0.

The amplitudes of thermally excited motions of a bilayer are microscopic. The mean square amplitude can be estimated (21): for capillary modes

$$\langle \zeta(q)^2 \rangle = \frac{k_B T}{\gamma_0 q^2 A}. \quad (14)$$

For a bilayer of diameter 4 mm, tension 3.5 dyne/cm and using $q = 1{,}300\ cm^{-1}$ (comparable to experimental values) the rms displacement is 0.02Å. The q value used corresponds to a wavelength $\Lambda = 48\ \mu m$, extending over some 10^5 lipid molecules (assuming an intermolecular spacing ~ 5Å). The fluctuation involves only tiny motions of the lipid molecules. The overall time average displacement of the membrane due to transverse fluctuations can be estimated by integrating Eq. 14 over q between physical limits (molecular separation $<\Lambda <$ BLM diameter). The average rms displacement thus found is ~3 Å, less than one-tenth of the membrane thickness.

Membranes of Anisotropic Molecules

A membrane comprising anisotropic molecules has more degrees of freedom available to it: fluctuations in intramolecular order and in molecular orientation become possible (22). Hitherto experimental studies of thermal fluctuations of model membranes (mono- or bilayers) have provided no evidence for the existence of these fluctuations.

The order parameter for uniaxial molecules in the BLM is the symmetric traceless tensor (see reference 23)

$$S_{ij} = S(3n_i n_j - \delta_{ij})/2, \qquad (15)$$

where S is a scalar quantity describing the degree of alignment of the lipid molecules and the unit vector $\hat{\mathbf{n}}$ describes the average orientation of the molecules (assumed normal to the BLM plane at equilibrium). Both S and $\hat{\mathbf{n}}$ are subject to thermal fluctuations, leading to order fluctuations and to twist and splay modes of the molecular orientation (Fig. 1). The order and splay modes couple to the fluctuations already discussed for the isotropic case.

The order fluctuations couple with the compression modes and the splay fluctuations couple with the transverse modes. For a symmetric membrane these two sets of modes are decoupled from each other, just as the transverse and compression modes are decoupled in the isotropic case. The dispersion equation for the splay-transverse vibration modes becomes (22)

$$i\omega - \left[\gamma + \frac{M(W + Kq^2)}{W + M + Kq^2}\right]\frac{q^3(q - m)}{2i\rho m\omega} = 0, \qquad (16)$$

where M expresses the coupling of the molecular orientation to the local BLM normal and K is the curvature elastic modulus (that governing splay) of the membrane. Normally W is zero for a BLM (22). For large M, the effect of this coupling upon the capillary waves is to increase γ_0 by Kq^2. Thus the capillary wave frequency (ω_0) is increased for given q, whereas the damping Γ is unchanged to first order (Eq. 7). The spectrum of light scattered by the coupled splay-transverse modes is unchanged *in form* from that for the capillary waves.

The intensity of light scattered by the transverse-splay modes (I_t) is also affected (22). For a symmetric membrane with molecular orientation tightly coupled to the local BLM orientation (i.e. M large),

$$\frac{1}{I_0}\frac{dI_t}{d\Omega} = \frac{\pi^2}{\lambda^4}\frac{k_B T}{Aq^2} \cdot \frac{[\mathbf{f}\cdot\mathbf{i}\, q_z\, h\, R_{s,p}^{1/2}(\epsilon_m - \epsilon_0) - \epsilon_a S_0 qh\,(i_x f_z + f_x i_z)]^2}{\gamma_0 + Kq^2}, \qquad (17)$$

where ϵ_a is the anisotropy of the dielectric constant of the BLM ($\epsilon_a = \epsilon_\parallel - \epsilon_\perp$, $\epsilon_m = (\epsilon_\parallel + 2\epsilon_\perp)/3$). The vectors $\mathbf{i}$ and $\mathbf{f}$ are the initial and final polarization vectors and components x and y are taken in the BLM plane, parallel and normal to $\mathbf{q}$, the wave-vector of the fluctuation involved in the scattering. The order parameter enters via its equilibrium value S_0. Eq. 17 has been adapted from Fan (22) by inclusion of the BLM reflectivity in the scattering by transverse motions. This equation shows that in some circumstances the molecular anisotropy results in a reduction in scattered intensity.

MATERIALS AND METHODS

Membranes

Bilayer membranes were formed under a 0.1 M NaCl solution from glycerol-1-monooleate (GMO). BLM incorporating substantial quantities of solvent (solvent membranes) were formed from solutions of GMO in *n*-decane. 'Solvent-free' BLM were formed from dispersions of GMO in squalane. In all cases lipid concentrations in the film-forming solutions were 10 mg/ml. The details of BLM formation have been described previously (5).

Membrane impurities are known to alter the characteristics of the lipid transition. Thus particular attention was paid to the purity of all the chemicals used. The suppliers (Pharmacia) quote the GMO purity as >99%, the oleic acid moiety being claimed 99+% pure. TLC tests with various solvent systems revealed only trace impurities (apparently free fatty acids and diglycerides). GLC on methyl esters of the lipid suggested the fatty acid constituent of the impurity was $C_{16:0}$, at a concentration below 1%. Independent GLC studies on GMO from the same supplier suggested the contamination by the 2-isomer was <0.5% (R. A. Klein, private communication). Consequently, GMO was used as supplied without further purification. Decane and squalane ('pure' grade, Koch-Light Chemicals) were purified using silver nitrate-alumina (24). The aqueous medium (0.1 M NaCl solution) comprised sodium chloride of 99.999% purity ('Gold Label' grade, Aldrich Chemical Co. Inc., WI) dissolved in 'polished' water (resistivity $1.8 \times 10^7\ \Omega$ cm) from a Milli Q filtration system (Millipore Corp). The solution was filtered through a 0.05 μm cellulose nitrate membrane filter and degassed before use.

The light scattering technique requires stable membranes that are of high quality and free from deformations from planarity. Many of the BLM formed were not of suitable quality and could not be used. 'Solvent-free' BLM appeared more planar than those incorporating decane. In this respect they were more suitable for light scattering studies, yielding data of higher accuracy. Unfortunately they were shorter-lived (4–5 h on average), making long experiments difficult. Data from solvent membranes showed random fluctuations, likely due to temporary local variations in membrane properties as microlenses of solvent in the membrane moved about. These fluctuations reduced the apparent precision of the technique for these BLM.

All membranes examined were subjected to the same experimental procedure. The film was formed at room temperature, well above the reported GMO phase transition, and allowed to drain for 2–3 h before light scattering work was started. Observations were then taken over several hours as the membrane was cooled slowly (<0.1°C/min) to below the accepted transition temperature. The temperature of the system was noted (±0.025°C) as each light scattering observation was started. Typically each such observation lasted 30 s, some two or three hundred correlation functions being recorded in a cooling run. If the membranes survived sufficiently long the process was continued in a heating run.

Light-Scattering

Light scattered at a well-defined small angle (<1%) from the specular reflection off the BLM was detected in a heterodyne spectrometer. Details of the apparatus and of its modification to provide sufficient resolution for phase transition studies have been published elsewhere (5, 12). Briefly, the membrane was illuminated by light from an Ar^+ laser (λ = 488 nm, TEM_{00} mode). The scattered light, together with light diffusely reflected from the membrane, was directed to the photomultiplier. Servo-controlled optics compensated for any changes in membrane orientation, ensuring negligible variations in the selected q value. The diffuse reflection provided a heterodyne reference beam. The photomultiplier output was analyzed by a multi-bit correlator (Malvern K7025). Measurements indicated that the laser beam was plane polarized (polarization ratio ~ 400:1) perpendicular to the plane of incidence. Scattering was detected in the plane of incidence. No restriction was placed upon the polarization of the scattered light collected by the detector. Heterodyne detection of depolarized scattering would only be possible if the reference beam were not fully polarized.

The heterodyne correlation functions observed could be represented by

$$G(t) = B + A\cos(\omega_0 t + \psi)\exp(-\Gamma t), \qquad (18)$$

where the phase term ψ accounts for deviations of the spectrum (Eq. 9) from the exact Lorentzian form (25). Fitting this form to the observed correlation functions yielded estimates of the amplitude of the time-dependent part (A), the bakcground (B) and the frequency (ω_0) and damping (Γ) of the surface fluctuations.

The frequency and damping observed for capillary waves of known q can be used to infer values of the viscoelastic properties of the system. The analytic approximations mentioned earlier could be used, but it is more accurate to substitute ω_0 and Γ into the dispersion equation as the real and imaginary parts of ω. The dispersion equation can then be solved for two physical properties. Initially we assumed $\gamma' = 0$ to derive values of γ_0 and η. If η was acceptably close to the known viscosity of the aqueous medium, γ' was considered to be negligible (see 5). If, however, η exceeded the accepted value, γ' was estimated by solving the dispersion equation for γ_0 and γ', while holding η equal to its accepted value. Tests with simulated data suggested that values of γ' thus derived were substantially more precise than those found using the higher order approximations (26).

The observed correlation functions corresponded very well with the form expected for thermally excited transverse fluctuations of the BLM. No extraneous scattering processes were evident on time scales comparable to or much slower than those appropriate to the transverse waves (25, 27). Very much faster processes could not be definitely excluded. Additional verification that the observed scattering arose from transverse fluctuations on the BLM was provided by the concurrence of the functional dependences upon q of ω_0 and Γ (5) and of scattered intensity (27) with those expected theoretically. Further, for solvent membranes the variations were entirely compatible with the behaviour predicted from the accepted value of η of the aqueous medium and from a membrane tension comparable with twice the bulk phase interfacial tension. As noted elsewhere (12), our present system yielded tension values comparable to membrane tensions, rather than interfacial tensions.

For molecularly anisotropic membranes, the membrane tension must be replaced by γ_{eff} ($= \gamma_0 + Kq^2$). All tensions reported below must be regarded as such 'effective tensions'. In principle, careful measurements of ω_0 and Γ as functions of q could indicate the effect of K upon γ_{eff}. Sufficiently precise measurements have not yet been carried out.

The correlator monitor channels provided an estimate of the total photon count rate (I_{tot}) and this, together with the amplitude to background ratio of the correlation function

$$\frac{A}{B} = \frac{I_s I_r}{I_{tot}^2}, \tag{19}$$

where

$$I_{tot} = I_s + I_r \; (I_r \gg I_s) \tag{20}$$

permitted estimates of I_s and I_r to be derived (27), despite the uncontrolled nature of the heterodyne reference beam. This derivation depends upon the presence of a single dominant scattering process in the system. Problems could arise in evaluating I_s and I_r if external vibrations coupled to the BLM. Such coupling has occasionally been evident in our experiments, observable as a long-time oscillation in the correlation functions. Any data showing such effects have been rigorously excluded from the present work. We believe that such gross disturbances do not influence the results reported below (see also 27). (The amplitude A (Eq. 18) should in principle contain a coherence factor, less than unity, (e.g. 62) which would modify I_s and I_r. For our experimental geometry this factor is close to unity (>0.97). It will be constant for fixed q, so that the *variations* of I_s and I_r inferred will not be changed. This factor is thus neglected here.)

Instrumental effects upon the form of the spectrum are well understood (25) and are negligible at sufficiently large q values ($\gtrsim$1,000 cm^{-1}, as in the present experiments). However, there are also effects upon the scattered intensity. The specular reflection from the BLM is observed to be diffuse due to deviations from planarity etc.: measurements of I_r as a function of q (27) suggest a reflected spot of Gaussian profile having $\sigma \sim$ 300 cm^{-1} (equivalent to 4 mm radius). This will lead to a similar spread in light scattered by a transverse fluctuation of fixed q (first term of Eq. 12). The detector pinhole (radius 0.2 mm) will accept only a small fraction ($\sim 10^{-3}$) of the intensity scattered by this fluctuation. Comparison of the calculated intensity scattered by the transverse waves with measured values confirmed this instrumental reduction. The scattering by compression waves (second term in Eq. 12) relates to fluctuations *within* a membrane (assumed planar) and will not be so affected. The net effect will be to rather reduce scattering by transverse waves compared to compression waves.

We report below data from a single BLM of each particular type. In all cases qualitative support was provided by data from similar membranes. Data from different membranes were not averaged, as results might vary slightly with the batch of GMO or solvent. As film-formation is not a very controlled process, the membrane composition may also vary slightly. For these reasons exact quantitative agreement is not to be expected, although transition temperatures observed for several BLM of similar type agreed to within 0.1°C. Many of the BLM studied did not provide data of good enough quality to justify detailed analysis. This likely arose from membrane variability.

RESULTS

GMO/Decane Membranes

There are two reasons for discussing experimental observations of GMO/decane membranes. Firstly, such BLM apparently have only a small membrane viscosity (if any) and thus the damping of the capillary fluctuations probed by light scattering can be compared with exact predictions based upon accepted η values (5). Such comparisons engender confidence in the experiment and the data interpretation. Secondly the transitions of these membranes offer illuminating comparisons with the 'solvent-free' case to be discussed below.

Frequency and damping data for a GMO/decane membrane taken through a complete temperature cycle from 22.1 to 9.9°C and back again are shown in Fig. 3. The changes in ω_0 and Γ with temperature arise from changes within the BLM and the ambient fluid. Arguments against an instrumental origin for these changes have been detailed elsewhere (12). The data at high temperature on the heating run coincide with those taken several hours earlier at the start of the cooling run.

The agreement between the heating and cooling runs permits the data of Fig. 3 to be averaged. Fig. 4 shows the tension (γ_0) and viscosity (η) values derived from ω_0 and Γ data averaged over intervals of 0.1°C. The smooth curve through the viscosity data shows the accepted T variation of η for 0.1 M NaCl (28). The observed η values follow the accepted trend reasonably closely (cf reference 5), suggesting that our experimental and analysis procedures are valid. At low T the observed data are systematically slightly below the accepted values. This is difficult to explain except by an error ($\sim$1.5%) in the q value used in the data interpretation. Such a small error is within the experimental precision. If the q value were corrected to ensure that η values at low T were scattered about the accepted line, the higher T data would slightly exceed that variation. Such a difference, while not large, might be indicative of a small but non-negligible membrane viscosity (γ') above $\sim$16.5°C. Such membrane viscosity—

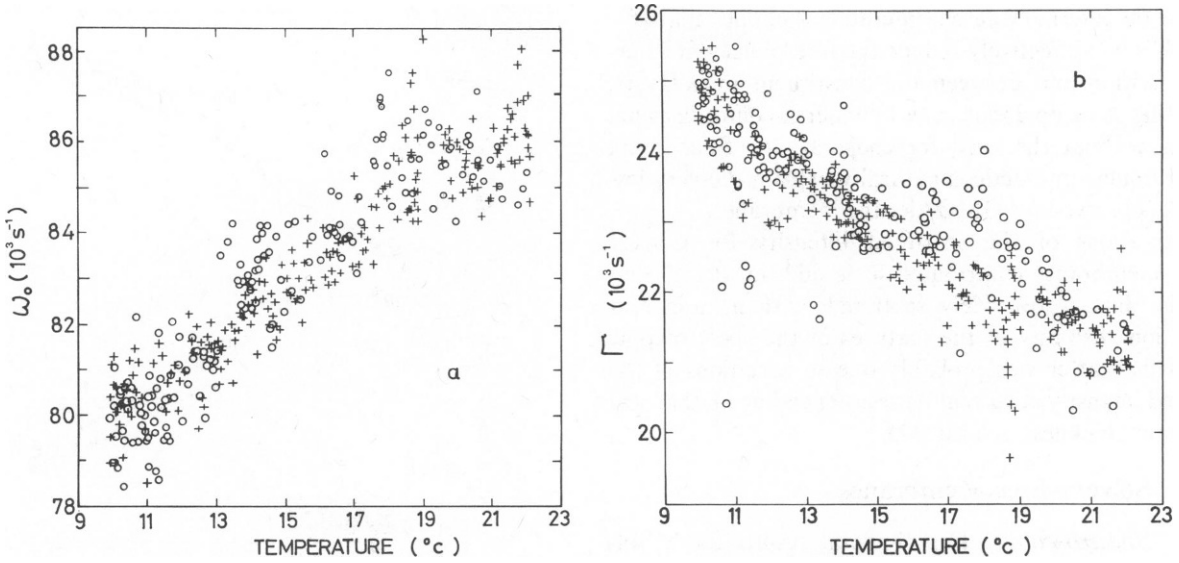

FIGURE 3 The frequency (ω_0) and damping constant (Γ) of capillary waves (q = 1,440 cm^{-1}) upon a GMO/decane membrane. Data is shown for a complete cooling (+) and heating (O) cycle.

perceptible at high T and falling to negligible levels at low T—is suggested by observations of GMO/decane membranes containing cholesterol (12) and by data for solvent-free BLM. We have not pursued such an analysis of the GMO/decane data because of the necessarily arbitrary nature of the correction to q.

The absolute tensions are comparable with literature values. The interfacial tension of a 3 mg/ml solution of GMO in n-decane against 0.1 M NaCl (29) suggests a membrane tension ~7.6 dyne/cm at 20°C (using $\gamma_{blm} = 2\gamma_{interf}$). Given the variation of γ_0 with lipid concentration in the film-forming solution (5) the agreement with the present data (~7.1 dyne/cm at a lipid concentration of 10 mg/ml) is very good.

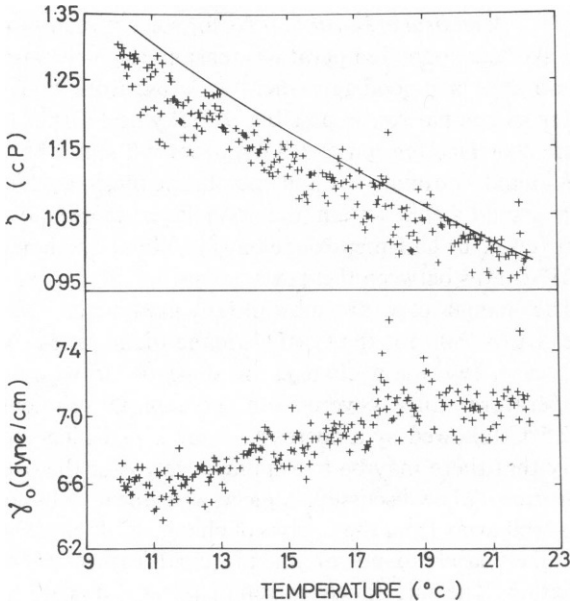

FIGURE 4 Viscosity of the ambient medium (0.1 M NaCl) and membrane tension inferred for a GMO/decane membrane (using Eq. 4). The line indicates the accepted temperature variation of viscosity.

The data of Fig. 4 confirm the positive $d\gamma_0/dT$ reported for bilayers (30) and for certain lipid monolayers at the oil-water interface (e.g. 31). The change in tension over the T range covered is small (~7%), and there are few relevant data for direct comparison. The interfacial tension of a solution of GMO in n/decane against 0.1 M NaCl increases at a rate of 0.034 dyne cm^{-1}/°C between 15 and 30°C (S. H. White, personal communication). The average gradient of the present data above 15°C is 0.039 dyne cm^{-1}/°C, in good agreement with this value.

The T variation of γ_0 (Fig. 4) is more complex than is implied by a single statement of slope. Between ~12 and 18°C the variation is faster than outside these limits. The behavior about 18°C resembles the variation of tension for lipid monolayers at an oil-water interface (31). While the present data are not sufficiently precise for any detailed interpretation, all GMO/decane membranes examined have exhibited such a double change in $d\gamma_0/dT$. There are some indications of a 'kink' in the tension data about 16°C, such as is more clearly perceptible in the 'solvent-free' BLM to be discussed below. However, there are no clearly evident discontinuities or sharp changes that could be associated unambiguously with a cooperative transition: a single transition temperature cannot be defined. Indeed it appears that the membrane transition extends over much of the T range examined, suggesting a rather low degree of cooperativity in the transition process.

GMO/decane membranes are known to retain substantial quantities of decane within the bilayer structure (32). The rather broad transition observed for these BLM may be explained by the effects of these solvent molecules. Hydrocarbon molecules within the BLM structure will

increase the internal volume (interactive volume) available (33). This will effectively reduce the intermolecular interactions within and between the constituent monolayers, permitting some lipid molecules to undergo conformational changes without the need for cooperativity. Such weak intermolecular interactions naturally explain the very low γ' values observed for GMO/decane membranes.

Observations of the scattered intensity for GMO/decane membranes contributed little additional information: the data were widely scattered, with no apparent correlation with any of the features of the spectroscopic data. This scatter was probably due to variations of the scattered intensity at solvent lenses (depending on the local membrane thickness, see Eq. 12).

Solvent-Free Membranes

Spectroscopy. Experimental results for a 'solvent-free' BLM formed at 25°C and cooled slowly to 7°C are shown in Fig. 5. The frequency of the capillary waves upon the membrane varies reasonably linearly with temperature. Some small systematic deviations from the line are evident between 12 and 18°C. However, the temperature-induced changes are more noticeable in the damping of the membrane fluctuations. At low T the measured Γ values are close to the variation expected from the accepted viscosity of 0.1 M NaCl. Above about 12°C the data depart markedly from these predictions.

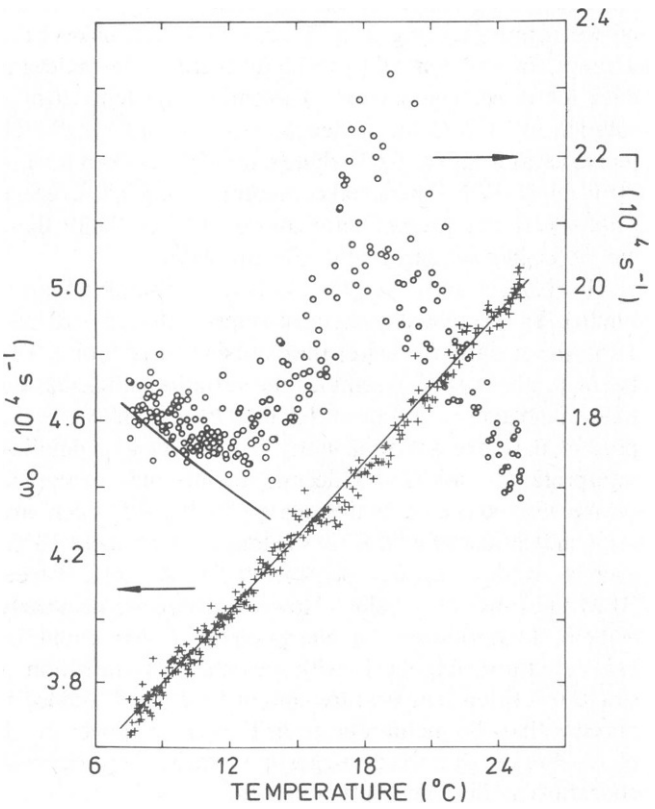

FIGURE 5 The observed frequency (ω_0) and damping constant (Γ) of capillary waves (q = 1,275 cm^{-1}) on a 'solvent-free' BLM. The line through ω_0 is a linear fit; that associated with Γ indicates the damping due to the viscosity of the ambient fluid. The Γ line extrapolates smoothly to higher temperatures.

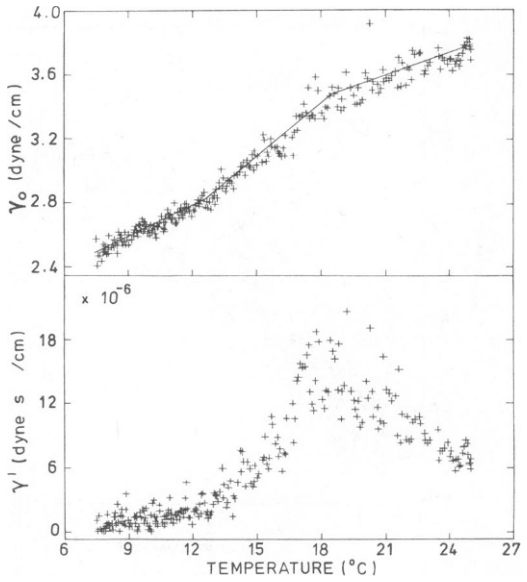

FIGURE 6 The membrane tensions (γ_0) and viscosities (γ') inferred from the data of Fig. 5 (using Eq. 4). The piece-wise linear fit to γ_0 is discussed in the text.

Values of γ_0 and γ' (Fig. 6) have been derived from the individual observed ω_0, Γ data, assuming that η followed its accepted variation. The plot of γ_0 is less linear than that for ω_0. The frequency ω_0 is predominantly determined by the tension γ_0, but the membrane viscosity γ' depresses the frequency expected for a given tension (5). The reasonably linear ω_0 variation thus results from the fortuitous cancellation of the effects of γ_0 and γ'.

Membrane Tension. As for solvent membranes, the average room temperature tension for 'solvent-free' membranes is in good agreement with literature values, in so far as comparison is possible. Hladky and Gruen (17) quote a surface tension of 1.5 dyne/cm but state that this should underestimate the half-membrane tension, which in turn should be less than the monolayer tension of 2.3 dyne/cm. Our half-membrane tension, about 1.8 dyne/cm at 21°C, falls between these two values.

The changes of γ_0 are substantially greater for 'solvent-free' BLM than for the GMO/decane membranes. As in that case, two main changes of slope occur within the temperature range covered: an increase in gradient at ~12.5°C followed by a decrease about 17.5°C. The possibility that there may be two stages involved in the overall transition will be discussed. A piece-wise linear fit based on data well away from the regions of change of slope is shown in Fig. 6, mainly to indicate the principal features of the γ_0 variation. The interfacial entropies ($S = -d\gamma_0/dT$) are shown in Table I. The data do not, however, demand two first-order transitions as would be implied by discontinuities in S: nonlinear functions could fit the data equally well.

Inspection of the residuals of this piece-wise linear fit reveals only one area of poor fit: systematic deviations occur between 15 and 18° (also seen in the ω_0 data, Fig. 5). These deviations are subtle but are observed for all membranes examined, both solvent and 'solvent-free.' Comparisons with data on membrane reflectivity for the same BLM (see below) permit the identification of this 'kink' in the γ_0 data with a transitional change and provide a precise value for T_t, 16.6°C.

Similar changes in slope have been observed for the interfacial tension of monomolecular films at oil-water interfaces (31). These latter data indicated a γ_0 variation approximating two straight lines, the higher temperature slope being smaller. The temperatures of the change of slope tended towards the accepted lipid transition temperatures as the lipid concentrations were increased. These changes were analyzed in terms of the enthalpy of fusion of the monomolecular film, evaluated by

$$\Delta H_f = \left(\frac{\partial H}{\partial A}\right)_l \frac{A_l}{A_s} - \left(\frac{\partial H}{\partial A}\right)_s, \qquad (22)$$

where A_l and A_s are the different areas occupied by lipid molecules in the fluid and solid phases and

$$\left(\frac{\partial H}{\partial A}\right)_{T,P} = \gamma_0 - T\left(\frac{\partial \gamma}{\partial T}\right)_{P,A}. \qquad (21)$$

This analysis, while originally applied to monolayers, translates in its entirety to lipid bilayers (see reference 30). The enthalpies shown in Table I were derived from the present data between 13 and 25°C using values of A_l and A_s for GMO given by White (9). The final enthalpy of fusion, ΔH_f is 277 cal/mol, far below typical values of the transitional enthalpy change (ΔH_t) deduced from calorimetric measurements on aqueous dispersions of lipids (e.g. 1). ΔH_f reflects the free energy changes due to changing lipid adsorption, whereas ΔH_t will include the energy required for conformational changes that only indirectly affect the adsorption.

Membrane Viscosity. The γ' data also show changes at certain temperatures, which correspond closely with the discontinuities in the γ_0 data (Fig. 6). Above about 17.5°C γ' decreases more or less smoothly with T. Below 12.5°C, however, it is essentially constant, close to zero (within the errors due to the precision of q). Above 12.5°C γ' increases smoothly to connect with the higher temperature variation. These γ' data may be considered from several rather different points of view.

TABLE I
ANALYSIS OF ENTHALPY OF FUSION OF BILAYER

T	S	$\partial H/\partial A$	A^*	$\Delta H‡$	ΔH_f
°C	*erg/cm²/°C*	*cal/cm*	Å²	cal/cm²	cal/mole
20	−0.0481	-2.52×10^{-7}	37	3.43×10^{-7}	277
14	−0.1107	-6.89×10^{-7}	27		
9	−0.0638				

*From White (9).
‡On the basis of molecular areas in solid phase.

For many bulk fluids viscosity falls approximately exponentially with increasing T. Moore and Eyring (34) showed that this behaviour should also apply to the surface viscosity (in-plane shear) of monomolecular films on liquid surfaces. If the arguments of Moore and Eyring can be extended to transverse shear, the high T variation of γ' is comprehensible. Motions of the lipid molecules are hindered by interactions between the fluid lipid chains, requiring activation over the barrier thus presented. At low T the small γ' suggests lipid molecules relatively free to move transverse to the membrane. At these temperatures, the lipid molecules thus appear to be aligned and comparatively rigid. The significance of the *cis* 9–10 double bond in the center of the GMO hydrocarbon chain, which would rather inhibit intermolecular motions, may be less than would at first appear because the thermal fluctuations of a given q value probed by light scattering are of very small amplitudes, so that only minutely small transverse shearing motions are involved. Between 12.5 and 17.5°C γ' shows a gradual transition between the two extremes.

An Arrhenius variation of viscosity seems most probable far from any phase transition, where purely kinetic activation may be expected, without any drastic changes in molecular interaction. However, close to a phase transition viscosity, like other dissipative response functions, is more likely to display characteristically transitional behavior.

Various theories of phase transitions of lipid systems have been developed in recent years. However, few, if any, treat the effects upon the membrane viscoelasticity. We have, therefore, sought theoretical treatments that are couched in rather general terms. Jahnig has treated various aspects of membrane transitions using a Landau approach (35, 36) and concludes that, while the transitions are first-order, they are 'almost second-order' in nature. Similar conclusions were reached by Doniach (37) for the specific case of ionic permeability.

Here only a brief sketch of this approach is appropriate, concentrating upon the observable consequences of the proximity of the membrane transition to a critical point. The main consequence is the appearance of fluctuations in the system. At a phase transition long-range order (for lipid bilayers the orientational order of the lipid chains) arises spontaneously. Using a Landau expansion the bilayer free energy can be expressed in terms of the scalar order parameter, S of Eq. 15:

$$f = -a_1 S + \tfrac{1}{2} a_2 (T - T^*) S^2 - \tfrac{1}{3} a_3 S^3 + \tfrac{1}{4} a_4 S^4 - \cdots, \qquad (23)$$

where T^* is the critical temperature of the membrane, and the coefficients are positive constants. The cubic term shifts the transition from a critical point at T^* to a first order transition at T_t ($>T^*$) at which the equilibrium

order parameter changes discontinuously. The order parameter fluctuates as T_t is approached. The fluctuations in S can be computed:

$$\langle |\delta S(q)|^2 \rangle \propto (T - T^*)^{-1} \; T > T_t$$
$$\propto (T_h - T)^{-1} \; T < T_t, \qquad (24)$$

where T_h is the high temperature inflexion point of $S(T)$. These 'pre-transitional' fluctuations, while characteristic of second-order transitions, do occur for first-order changes, being rather less pronounced. The fluctuations at a first-order transition display the classical critical exponents of Eq. 24 as T_t is *relatively* far from T^*, in the so-called classical regime (35). Such pretransitional effects should also be evident in the response of the system to external perturbations (35). It should be noted that these pretransitional fluctuations have nothing to do with the so-called pretransition (here called 'the lower transition' for clarity) observed for dispersions of phospholipids in water but rather reflect the ease with which fluctuations can arise close to critical points.

The data of Fig. 6 are strongly suggestive of such behavior: a first-order transition rather close to a critical point. The tension data of Fig. 6 show a rather small change at T_t (i.e. the 'order parameter' changes only slightly); considerable pretransitional effects appear in the response function (γ'). The inter-relation between γ and orientational order in the membrane is somewhat ill-defined, but the dissipative response function γ' clearly reflects a pretransitional increase in fluctuations of the order parameter.

The γ' data of Fig. 6 were analyzed using Eq. 24, for $T > T_t$ and $T < T_t$, separately. In both cases data within the transition region (15.8 to 17.4°C) was omitted. Due to the scatter on the γ' data the values of T^* and T_h inferred in this fitting process were somewhat dependent on the exact data points used in the fitting procedure. The analysis was therefore repeated several times, shifting the lower (upper) limit of the high (low) temperature data systematically up (down) by one point at a time. The fit to the high temperature data was remarkably constant, giving T^* = 12.7°C to within 0.4°C as data points between 18.5 and 19.4°C were progressively eliminated. The fit to the low temperature data was much less stable, a constant value of T_h = 16.8°C (to within 0.1°C) being obtained only as points between 15.5 and 15.8°C were dropped. Inclusion of data closer to T_t for this low temperature data caused the fit (judged by both the sum of squares and the runs of the residuals) to deteriorate significantly. Thus, while the value T^* = 12.7°C seems well-founded, T_h = 16.8°C is rather less certain.

Fig. 7 shows the best-fit functions of the form of Eq. 24 together with γ' averaged over intervals of 0.5°C (the original data were of course used in the fitting process). As T decreases in the fluid phase the free energy falls as if approaching a second-order transition at T^*. Before reaching T^*, however, the actual first order change supervenes. Similarly, in the ordered phase, the free energy falls as T increases as if another second order transition at T_h were being approached. Again the actual transition occurs at T_t, preempting this variation. The free energy associated with fluctuations in S about its equilibrium value falls as T_t is approached, causing the 'pre-transitional' fluctuations in the order parameter.

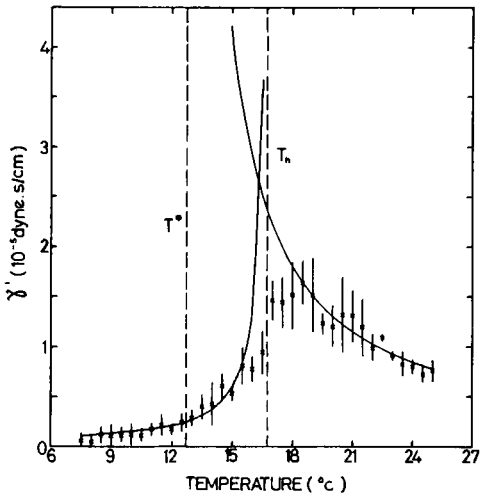

FIGURE 7 Membrane viscosity, averaged over 0.5°C intervals, compared to best-fit functions of the form of Eq. 24. The asymptotes of these functions are indicated by dashed lines at T^* and T_h.

Finally, the viscoelastic modulus γ ($= \gamma_0 - i\omega\gamma'$) that governs the thermally excited transverse waves of the membrane can be analyzed to yield a characteristic relaxation time. As ω increases from zero so the imaginary part of γ increases, ultimately exceeding γ_0. Increasing the effect of the dissipative γ' relative to the driving force of tension will ultimately lead to overdamping of the waves. We define the relaxation time τ as

$$\tau = 1/\Omega = 1/(\gamma_0/\gamma'), \qquad (25)$$

Ω being a frequency such that the real and imaginary parts of γ are of equal magnitude. Such a relaxation time determines the time-scale of the fluctuations of that order parameter relevant to the transverse shear motions. Fig. 8 shows τ as a function of T, averaged over intervals of 1.0°C.

Five time scales characteristic of different processes occurring in the lipid phase transition have been identified in a study using an iodine-laser T-jump technique (38). These time scales range from a few ns to 10^{-2} s, corresponding to different stages in the transition process, from the non-cooperative formation of kinks in the lipid hydrocarbon chains to the strongly cooperative destruction of ordered clusters. The cooperativity of each process was judged by the sharpness of the corresponding transitional peak (38). The observed time scale $t_3 \sim 10^{-5}$ s was associated with the cooperative formation of *gauche* con-

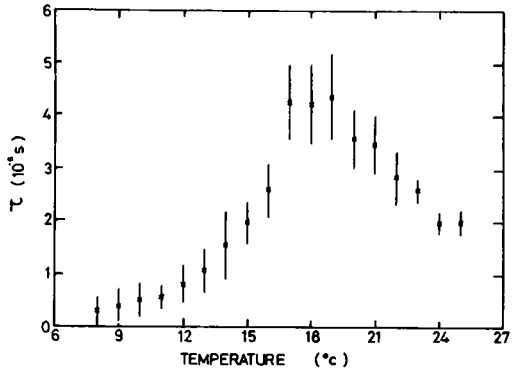

FIGURE 8 Relaxation time τ ($= \gamma'/\gamma_0$, data from Fig. 6) associated with transverse fluctuations of the membranes. Values shown are averaged over intervals of 1.0°C.

formations in the hydrocarbon chains. The data of Fig. 8 are similar to this t_3, both in cooperativity and in absolute magnitude. The appearance of *gauche* conformations will change the lipid head group separation, altering the tension.

This assignation is supported by the effects of cholesterol upon the relaxation time τ. Published data for ω_0 and Γ for GMO/decane membranes incorporating cholesterol (12) show transitional effects rather similar to those reported here for 'solvent-free' BLM. The cholesterol data lead to a rather less cooperative behavior for τ and a reduced peak value ($\sim 3 \times 10^{-7}$ s). Eck and Holzwarth (39) found that the addition of cholesterol to membranes caused such faster relaxation and lower cooperativity due to uncoupling of the hydrocarbon chains in the apposed monolayers.

Having identified one time scale in the present data, the question arises whether other time scales could be detected by such experiments. Very much faster relaxation processes could not be observed by the present light scattering techniques: much more precise ω_0 and Γ data, together with an exact determination of q, would be needed to perceive the effects of $\gamma' \ll 10^{-6}$ dyne.s/cm. However, it does appear that any relaxation processes much slower than 10^{-5} s that may occur in the transition are not involved in the response to transverse shear stress.

Intensity Measurements

The correlation data can provide further information (27) concerning light intensities (expressed here as photodetection count rates). These are derived from the amplitude:background ratio (A/B, Eq. 19) and the mean count rate (I_{tot}, approximately I_r, Eq. 20), both shown in Fig. 9. A/B abruptly decreases at ~12°C, and increases more gradually towards 18°C. These changes appear to arise primarily from I_{tot} rather than from the scattered intensity.

These data yield I_r and I_s as functions of T (Figs. 10 and 12). The results are noisy, as our experiments were not optimized for intensity measurements. The basic assumption, that no extraneous scattering processes occur, appeared well founded for *all* the present data: the observed correlation functions always had flat backgrounds that agreed well with the background at infinite time computed from the correlator monitor channels and were always of the form theoretically expected. We can definitively exclude any processes having time scales slower than or comparable to the transverse waves but not those so fast that the time dependence is averaged out within one correlator sample time (typically 5 μs).

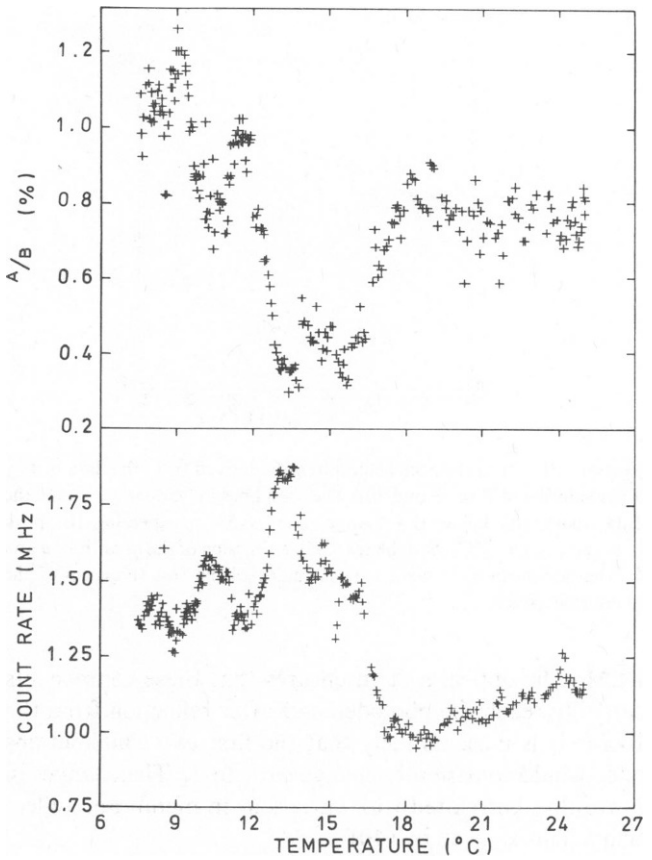

FIGURE 9 The ratio amplitude: background (A/B) of the observed correlation functions and the mean photodetection count rate (I_{tot}).

Reference Beam Intensity. It is convenient to discuss I_r first. This displays a considerable peak between 12 and 14°C, which will be discussed below in detail: briefly we associate it with the appearance of another process. Leaving aside this peak, I_r increases slowly with T from 7°C until a sudden decrease about 16.5°C, after which a slow increase is again evident. The fluctuations that are visible, particularly below 16°C, do not obscure these trends. The lines on Fig. 10 are the best-fit straight lines to the I_r data below and above the sudden change (omitting the peak between 12 and 14°C from the fit).

The reference beam (I_r) arises from flare from glass components, from scattering by quasi-static 'particles' in the aqueous medium and from diffuse reflection from the

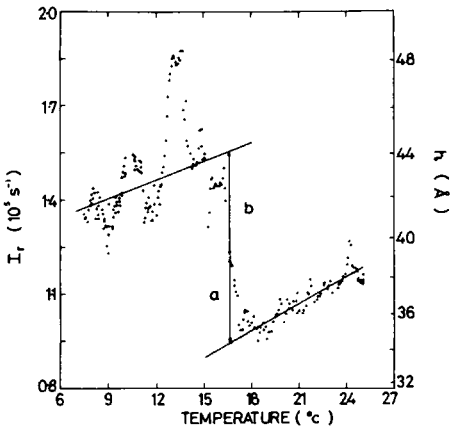

FIGURE 10 The reference beam intensity derived from the data of Fig. 9 (by solution of Eqs. 19 and 20). The solid lines indicate linear fits to the data above and below the change near 16.5°C (neglecting the peak between 12 and 14°C). See the text for a discussion of the quantities *a* and *b*. The nonlinear *right-hand* scale *h* indicates the rms thickness of the membrane (see text).

BLM. The optical system ensures that these components can only reach the photodetector after reflection from the BLM. It is most unlikely that the first two contributions cited would consistently change close to T_t. The changes in I_r are thus correlated with variations in membrane reflectivity. This is given by (40)

$$R = [2\pi(n_m - n_0 + \Delta)h/\lambda]^2 \quad (26)$$

where

$$\Delta = (n_m - n_0)^2/(n_m + n_0), \quad (27)$$

h is the membrane thickness, n_m the mean refractive index of the membrane, and n_0 the refractive index of the aqueous phase. As both n_m and n_0 can be taken as constant (see below), $I_r \propto h^2$.

We associate the sharp change in I_r at ~16.5°C with a change in BLM thickness. Other explanations are less likely. Solvent lenses might arise at membrane transitions but have never been observed (by ourselves or by other workers) for 'solvent-free' BLM. Rippling of the membrane, as observed between the main and lower transition in bulk dispersions of phospholipids (41), would increase the diffuse reflectance. However, it is known that single bilayers adopt planar configurations (17). Also lipid molecules with small head-groups (such as GMO) should preferentially orientate normal to the membrane plane (41) and indeed, as this would imply, no lower transition has been observed for mono-glycerides (8). We thus discount the possibility of rippling.

Variations in reflected intensity at lipid transitions have been reported previously. Analysis of the abrupt reflectivity changes observed (8) as single BLM formed from glycerol monostearate in n-hexadecane were cooled through the transition (as determined by DSC) showed that h increased from 45 ± 1Å to 77 ± 4Å at T_t, whereas n_m remained unchanged (within experimental error). We will return to the apparent constancy of n_m.

The data of Fig. 10 permit the rms thickness h to be deduced as a function of T (assuming constant n_m). From membrane reflectivity measurements Dilger (42) has determined h = 36Å at 20°C for a 'solvent-free' BLM formed from a 3 mg/ml dispersion of GMO in squalene. Using this calibration datum and assuming $I_r \propto h^2$, we derive the thickness scale shown in Fig. 10. The observed change in h at ~16.5°C is 8 Å. The BLM thickness at 16°C is therefore ~44Å, in excellent agreement with a value of 44.6Å suggested for a bilayer of fully-extended GMO molecules orientated normal to the membrane (9). At present we concentrate upon the changes close to 16.5°C. The slow temperature variations in h^2 will be discussed below.

An 'order parameter' ϕ appropriate to the changes in I_r (or h^2) can be defined (see reference 43). The differences (a and b) of the data within the transition region from the extrapolated linear variations shown in Fig. 10 enable this order parameter to be estimated:

$$\phi = a/(a + b). \quad (28)$$

The order parameter varies through the transition region as shown in Fig. 11, the transition temperature being defined as the temperature for which $\phi = 0.5$. A value T_t = 16.6 ± 0.03°C is found. Hereafter, reference to T_t will imply this value. The data of Fig. 11 are very close in form to $erf(T - T_t)$ with standard deviation σ = 0.6 ± 0.02°C ($\Delta T_{1/2}$ = 1.5°C). The transition thus appears quite sharp and symmetrical, at least as evidenced by these changes in membrane reflectivity. Unfortunately the lack of a value for ΔH_t prohibits estimation of the size of the cooperative unit.

The order parameter is plotted in Fig. 11 as $(1 - \phi)$ to facilitate comparisons with the variation of γ_0. The slight

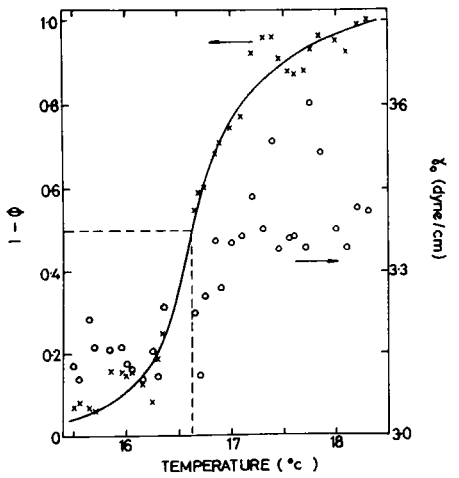

FIGURE 11 The variations of the order parameter ϕ (x) derived from the change in I_r at ~16.5°C. Values of membrane tension (o) are also plotted.

kink evident in the original plot of γ_0 (Fig. 6) coincides closely with the T_t as inferred from ϕ, the temperature variations of γ_0 and ϕ following very similar courses. The kink in γ_0 thus appears to be real and associated with the membrane transition.

We now return to the slow variations of I_r away from T_t. The present data indicate that dh^2/dT is 25Å^2/°C between 7 and 15°C and 37Å^2/°C between 18 and 25°C. These positive gradients are somewhat unexpected, although there are very few, if any, reports of measurements of dh/dT for BLM. Even for multi-lamellar systems only the transitional change in h has been reported (e.g. 45). Theoretical arguments (e.g. 44) based upon molecular conformational changes suggest an essentially constant membrane thickness below T_t and a negative temperature gradient above that point, as the lipid chains become more disordered and hence, on average, shorter. These theoretical thermal expansion coefficients have been compared (44) with the average bulk thermal coefficient measured for multi-lamellar lipid dispersions, showing some measure of agreement. This conflict with the present results is more apparent than real, as the systems are rather different. The perturbation due to the inter-lamellar forces (e.g. 4) may well overwhelm an intrinsic increase in membrane thickness on heating.

A positive dh/dT is compatible with the observed T dependence of the capacitance (C) of single GMO membranes (9). C generally decreased with increasing T for BLM formed from GMO dissolved in various solvents; in some cases the gradient changed at ~16°C. The specific geometric capacitance of the BLM is (using ϵ_0 for the permittivity of free space)

$$C_g = \epsilon_m \epsilon_0 / h \qquad (29)$$

so that (for constant ϵ_m – cf n_m [8]) a negative dC/dT implies a positive dh/dT. These capacitance observations, taken together with our I_r data, substantiate the reported lack of variation of n_m for monoglyceride BLM (8). Both C_g and R increase with n_m (Eqs. 26, 29), so that the opposite signs observed for dC/dT and dI_r/dT support the constancy of n_m over the T range covered (8). Therefore the variations of C and I_r must arise from changes in h. It should be noted that the change in h at T_t cannot easily be estimated from these studies of C: either the membranes contained quantities of solvent or the transitional region was confused by the proximity of the solvent melting point.

It is not immediately obvious why single BLM slowly increase in thickness on heating (away from T_t). White (33) suggests that the average membrane thickness might be influenced considerably by random fluctuations of a few lipid molecules from a *gauche* conformation to the fully-extended all-*trans* state. Above T_t this might well cause a positive dh/dT, but just below T_t our rms value for h (~44Å) is already close to twice the length of a fully extended GMO molecule. While below T_t the GMO molecule is slightly lengthened if the terminal *trans* bond of the hydrocarbon chain transforms to a *gauche* bond (46), neither the overall average temperature variation of I_r below T_t nor the fluctuations in that region can easily be explained by White's mechanism. Theoretical treatments of the membrane thickness (e.g. 44) ignore the possibility of temperature-dependent interactions within or between the two monolayers of the BLM. Any changes in intermolecular forces will modify the potential $U(h)$ and may alter the equilibrium thickness of the membrane. For example the increasing probability of *gauche* conformations above T_t will increase steric forces, increasing d^2U/dh^2. The present observations are compatible with an increase in the mean square amplitude of thickness fluctuations (17) since both γ_0 and d^2U/dh^2 increase with temperature. The increased gradient of I_r above T_t is likely to reflect the greater flexibility of the melted lipid chains.

Scattered Intensity. The observed I_s (the *measured* intensity scattered by capillary waves, found by solving Eqs. 19 and 20) is shown in Fig. 12. Within the range 12–14°C values of I_s were derived using I_r from the linear variation shown in Fig. 10. The I_s values thus determined agreed excellently with adjacent results (see Fig. 12). Other procedures destroyed this agreement.

Given the T dependences of h^2 and of γ_0 the *theoretical* variation of the intensity (I_t) of light scattered by transverse fluctuations of a membrane comprising isotropic molecules can be calculated from the first term in Eq. 12 (16). The piece-wise linear descriptions of γ_0 (Fig. 6) and h^2 (or I_r, Fig. 10) give I_t shown by the solid lines in Fig. 12, normalized to I_s at 24°C. Between 15.4 and 17.8°C (2σ range from T_t) the expected behavior is approximated by

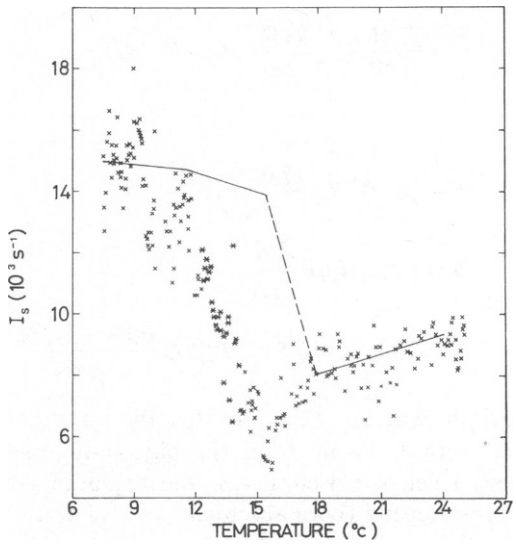

FIGURE 12 The scattered intensity I_s (x) derived from the data of Fig. 9 (solving Eqs. 19 and 20). Data derived using interpolated values of I_r between 12 and 14°C are distinguished (*). The line indicates the variation of I_t predicted by Eq. 10 for a membrane of isotropic molecules.

the dashed line. The observed data (I_s) agree excellently with the predictions (I_t) above the transition region. Below 18°C a marked divergence appears over a wide temperature range, the agreement becoming reasonable again below ~9°C. These observations could arise from a substantial decrease in n_m over a limited T range but this would be incompatible with other observations (8, 9).

Constraints are placed upon explanations for this discrepancy as I_s derives from the amplitude of the time dependent part of the observed correlation functions. We have already noted that this time dependence accords well with that expected for transverse membrane fluctuations. Thus any mechanism postulated to explain the deviation of I_s from the expected behavior must involve processes closely coupled to the transverse fluctuations so that the overall spectrum of the scattered light does not deviate from that of the transverse waves. This argument eliminates uncoupled membrane modes, such as thickness fluctuations, which could scatter light.

The essential elements of an explanation appear in Fan's treatment of the scattering of light from a membrane of optically anisotropic molecules (22). The transverse waves couple to fluctuations of the molecular splay: we shall consider the case of molecular axes strongly coupled to the local membrane normal. One effect is to increase the membrane tension by a term Kq^2, the other, of present concern, is to modify the scattered intensity (see Eq. 17). The exact change in I_s depends upon polarization factors and the relative magnitudes of ϵ_m (mean membrane dielectric constant) and the product $\epsilon_a S_0$ (anisotropic part of the dielectric constant and equilibrium order parameter).

The expression (Eq. 17) for the intensity scattered by the coupled splay-transverse vibration modes upon a symmetric membrane can be expanded as

$$\frac{1}{I_0}\frac{dI}{d\Omega} = \frac{\pi^2}{\lambda^4}\frac{k_B T h^2}{A}[E + F - G], \tag{30}$$

where

$$E = (\mathbf{f}\cdot\mathbf{i})^2 R_{s,p}\frac{[q_z(\epsilon_m - \epsilon_0)]^2}{\gamma_0 q^2}$$

$$F = (i_x f_z + f_x i_z)^2 \frac{\epsilon_a^2 S_0^2}{\gamma_0} \tag{31}$$

$$G = 2(i_x f_z + f_x i_z)(\mathbf{f}\cdot\mathbf{i})\, R_{s,p}^{1/2}\, q_z \frac{(\epsilon_m - \epsilon_0)\,\epsilon_a S_0}{\gamma_0 q}.$$

Comparison with Eq. 12 shows that the term E here is identical with I_t. Aside from the physically interesting variations which may occur in $\epsilon_a S_0$, the magnitudes of these three terms depend (both absolutely and relatively) upon the reflectivity, an instrumental factor already discussed (not shown explicitly in Eq. 31, but affecting the terms E and G similarly to $R_{s,p}$) and the polarization states of the incident and scattered light. These factors were all somewhat ill-determined in our experiment. However, we estimate that the combined reflectivity ($R \sim 10^{-5}$) and instrumental factor ($\sim 10^{-3}$, see above) reduced E by $\sim 10^{-8}$ (and hence G by 10^{-4}). The exact value is of little consequence as it simply combines with the polarization factor

$$X = \frac{(i_x f_z + f_x i_z)}{\mathbf{f}\cdot\mathbf{i}}. \tag{32}$$

For the case of light plane polarized in the s state incident upon the membrane the terms F and G in Eq. 30 vanish. However, measurements suggest that the extinction ratio of the beam actually reaching the BLM might have been $\lesssim$50:1. Slight variations of the membrane orientation could alter the polarization factor. For an extinction ratio of 50:1 and our experimental geometry the factor X would be ~0.02.

We have computed the intensity terms which involve the molecular anisotropy (F and G) relative to the dominant term (E) for various polarization factors. Fig. 13 *a* shows these terms as functions of $\epsilon_a S_0$ for various X values (found using a value of 10^{-8} for the combined reflectivity/instrumental factor). For small polarization factors both F and G are negligible compared to E. For $X = 0.01$ the combination $(E + F - G)$ is always less than E alone ($\epsilon_a S_0 > 0$). At relatively large X (e.g. 0.05) the contributions F and G are significant (Fig. 13 *b*): at low values of $\epsilon_a S_0$ the total scattered intensity is substantially decreased ($G > F$) whereas for large $\epsilon_a S_0$ the scattered intensity is increased ($F > G$).

Any choice of a specific value of X is essentially arbitrary as the exact initial and final polarization states were not defined during the present experiments, nor was

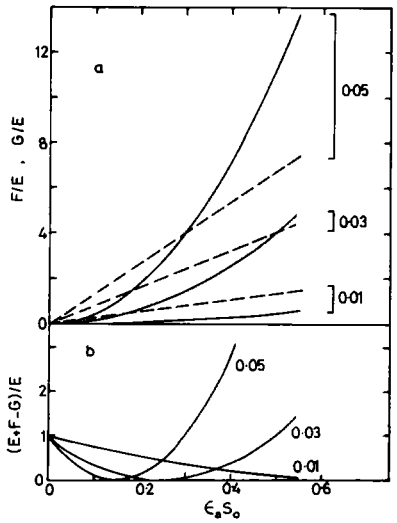

FIGURE 13 Effects of molecular anisotropy upon the intensity scattered by splay-transverse fluctuations. (*a*) Terms F (—) and G (---) from Eq. 30 plotted relative to E (= I_t). (*b*) The combined intensity $(E + F - G)$ plotted as a fraction of E. The parameter of the curves is the polarization factor, X.

the combined reflectivity and instrumental factor definitely established. While this leads to difficulties in establishing *absolute* values of $\epsilon_a S_0$ from our results, we can be confident of the *form* of the temperature variation of $\epsilon_a S_0$ that would account for the observed I_s data.

From Fig. 12 the differences between the observed I_s values and the predicted variation of I_t can be estimated (as $[I_t - I_s]/I_t$). Comparisons with curves such as those of Fig. 13 *b* permit estimation of the variation of $\epsilon_a S_0$ (Fig. 14, deduced using $X = 0.03$) required to explain the observed I_s data. Other choices of polarization factor change the absolute values of $\epsilon_a S_0$ but do not alter the form of the variation. This form is clearly suggestive of a transitional change close to 15.5°C. The apparent sharpness of the transition is independent of the value of X.

The normalization of the theoretical I_t variation to the observed I_s data at high temperature (T = 24°C) necessarily matches I_t to I_s in this region and hence forces $\epsilon_a S_0 = 0$ here. However, this feature is an artefact of our analysis. The lipid orientational order parameter is known to be nonzero in the fluid phase (for phospholipids $S_0 \sim 0.7$, [47]) and even at high temperature the lipid molecules are somewhat anisotropic (42). The value of $\epsilon_a S_0$ at high temperature may be estimated to be ~0.09 (see below).

The agreement of the observed I_s values with the expected variation (I_t) at $T \lesssim 9$°C is apparently fortuitous. The variation of $\epsilon_a S_0$ shown in Fig. 14 could lead to $I_s > I_t$ at low T. The lack of I_s data below 7°C has prevented verification of this prediction.

Since $\epsilon_a S_0$ is a double valued function of $(E + F - G)$ for all but the smallest values of X (see Fig. 13 *b*) other variations of $\epsilon_a S_0$ could be invoked to explain the data. For example, as T decreases $\epsilon_a S_0$ could increase to ~0.1 at 15.5°C followed by a drop to zero. The variation shown in Fig. 14 is preferred for its physical plausibility.

The uncertainties in this interpretation of the data on scattered intensity could largely be eliminated by further experiments involving precisely specified initial and final polarization states (i and f) and measurements of depolarized scattering.

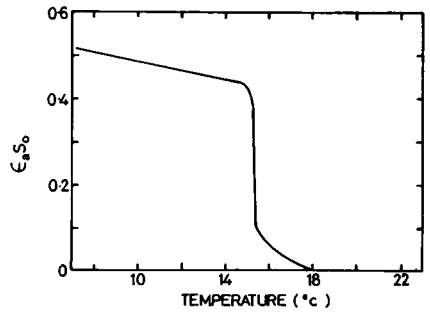

FIGURE 14 The variation of $\epsilon_a S_0$ (the anisotropic dielectric constant combined with the orientational order parameter) required to account for the observed behavior of I_s (Fig. 12). The polarization factor was taken as $X = 0.03$.

Compression Waves. We return to the substantial peak in I_r between 12 and 14°C (Fig. 10), which basically reflects the corresponding feature in the average photodetection count rate, I_{tot} (Fig. 9). Now I_{tot} is the total photodetection count rate, due to the reference beam and to light scattered by all processes occurring in the scattering system. If the transverse fluctuations of the BLM are the only scattering process present the analysis outlined earlier yields values of I_r and I_s that behave consistently (see Figs. 10 and 12 away from 12–14°C) (also 27). Between 12 and 14°C the analysis of A/B and I_{tot} in terms of I_r and I_s breaks down: the I_r values deduced are excessively large (see Fig. 10) and the I_s values would be too small unless corrected I_r values are used. An extra scattering process causing scattered intensity I_c would imply

$$I_{tot} = I_r + I_s + I_c. \tag{33}$$

We have seen that replacing I_r in the analysis for I_s between 12 and 14°C by values deduced from the linear interpolation of Fig. 10 leads to values of I_s entirely compatible with results at neighboring temperatures (Fig. 12). This suggests that the peak in the observed I_r data (Fig. 10) indeed arises from another scattering process, contributing to I_{tot} as in Eq. 33. Below 12°C I_r displays fluctuations; these appear to be real variations in the reference beam intensity. The values of I_s inferred using these measured I_r values do not display corresponding fluctuations in this region (Fig. 12), unlike between 12 and 14°C.

I_c can be extracted from I_{tot} in the region 12–14°C using Eq. 33, taking the linearly interpolated I_r (Fig. 10) and the observed I_s values (Fig. 12). This analysis procedure forces I_c to zero outside this T range. In reality, while such an extraneous process might cause negligible scattered intensity, I_c would never become identically zero. This error slightly affects the values of the membrane properties underlying the extra scattering process and necessarily restricts the T range accessible.

Compression (density) modes in the membrane plane provide the most likely explanation for I_c. Thickness fluctuations in 'solvent-free' BLM are only significant for q values much larger than that used experimentally (17). Changes in diffuse reflectance from the membrane (or any other static process) might occur, but would contribute to the heterodyne reference beam: the peak in Fig. 10 is *not* part of the reference beam intensity.

Eq. 13 relates the ratio of the *theoretical* intensities scattered by transverse and compression modes of the membrane (I_t/I_c) to the ratio of the in-plane compression modulus to the tension of the membrane (e_0/γ_0). In general for BLM far from a transition γ_0 is low, e_0 is large and I_t dominates I_c. This is the case in the present data for $T <$ 12°C and $T >$ 14°C. However, between 12 and 14°C the scattering by density waves dominates. Eq. 13 permits e_0 to

be estimated, knowing I_t, I_c, and γ_0. Other quantities in Eq. 13 are known constants: at 20°C $\epsilon_m = 2.20$ (42) and $\epsilon_0 = 1.788$ (48), $q = 1{,}275\ cm^{-1}$ and $q_z = 2.30 \times 10^5\ cm^{-1}$ from experimental geometry:

$$q_z = 4\pi/\lambda\ [\cos\theta + \cos(\theta + \delta\theta)]. \quad (35)$$

Any slight changes of dielectric constant with temperature might refine the value of e_0 but will not alter the general variation radically. The combined reflectivity and instrumental factor was again taken as 10^{-8}. In forming the ratio I_t/I_c, I_t was evaluated from the line of Fig. 12, as Eq. 13 neglects the molecular anisotropy which affects the observed I_s values. The temperature variation found for e_0 is shown in Fig. 15. The *form* of the temperature variation of e_0 is quite well-established but the absolute values are rather uncertain (as for $\epsilon_a S_0$).

The compression modes scatter light strongly over the region 12–14°C and might be expected to contribute an observable time-dependence to the correlation functions. However, using Eq. 8, the approximate frequency corresponding to the minimum value of e_0 in Fig. 15 (~3 kdyne/cm) is found to be 8.4 MHz. The time dependence of a fluctuation of this frequency would be completely averaged out within a single correlator sample time (~5 μs in these experiments). The compression modes are also very rapidly damped ($\Gamma \sim 4 \times 10^{-6}\ s^{-1}$). Even large decreases in the absolute values of e_0 would not cause the compression waves to have frequencies observable in our experiments.

A drop in membrane lateral compression modulus (e_0) close to a lipid phase transition has been suggested before.

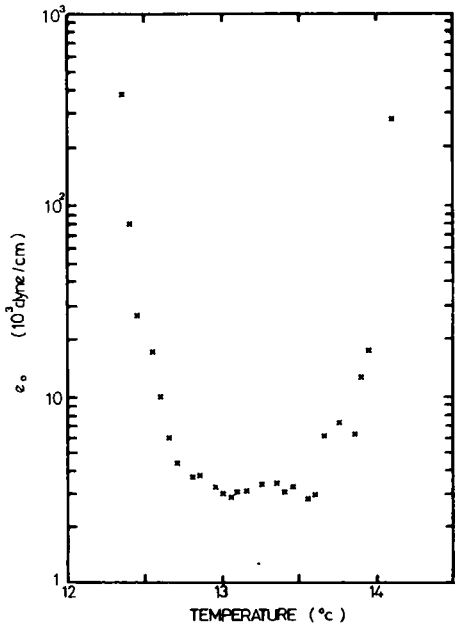

FIGURE 15 Values of the compression modulus derived from the peak in I_r (Fig. 10) between 12 and 14°C, using Eq. 13 and the observed variation of γ_0 (Fig. 6).

Theoretical treatments of the transitional increase in membrane permeability (49, 50) have predicted a variation of e_0 in general accord with the form of the present results. Measurements on DMPC bilayer vesicles showed a transitional peak in the elastic area compressibility ($1/e_0$) coincident with the accepted T_t (60). Both the theoretically predicted values of e_0 and those inferred from these measurements are very much lower at the transitional minimum than the data of Fig. 15.

The present results are not in very good accord with other measurements of bilayer compression moduli (51, 7). The discrepancies between the results may simply reflect the different model systems (differences in packing, geometry, open vs. closed systems, inter-bilayer forces), different lipid head groups and the effects of mixed lipid compositions (7). However, the major source of differences is probably the uncertainty in the present absolute values of e_0 arising from the ill-determined combined reflectivity and instrumental factor.

While for most interfacial systems compression waves will cause negligible scattered intensity compared to the capillary waves (16), this is not the case for BLM in the transitional region. In this system the spectrum of light scattered by compression waves should be measurable. Such observations would permit e_0 (and possibly e') to be determined directly, removing the ambiguities of the present approach.

DISCUSSION

The Nature of the Transition in GMO

Earlier studies on GMO bilayers are briefly reviewed below, preceding a discussion of the information from the present study. Transitional changes have previously been demonstrated in GMO over a range of temperatures (~12 to ~17°C) but little information has emerged upon the nature of the transition.

The calorimetric observations of Pagano et al. (8) have usually been cited as evidence of a lipid chain-melting transition. In these studies of lipid/hexadecane/water systems a peak at 15.2°C was only observed in the presence of GMO. This peak was attributed to a lipid phase transition in GMO, but the transitional temperature is close to the freezing point of hexadecane and may be influenced by the binary nature of the system investigated. These difficulties have been pointed out by R. A. Klein (private communication), who recently studied GMO/water as a control. A transitional peak was observed about 15°C, but, rather abnormally, only on the heating part of the temperature cycle. Capacitance studies of BLM formed from GMO in various solvents (9) suggested organizational changes in the GMO molecules between 15 and 20°C, and perhaps between 5 and 10°C. These C changes correlated with changes in the interfacial tension of a solution of GMO against water between 15 and 18°C. Fahey and Webb (10) studied BLM formed by both the Montal-Mueller (MM)

method (giving solvent-free membranes) and the Mueller-Rudin (MR) method (solvent type membranes). The lateral diffusion coefficient of a fluorescent probe (diI) in MM membranes slightly increased between 10 and 16°C, whereas the MR type showed no significant change. A much more distinct change occurred in fluorescence intensity measurements (for M540) at ~12.8°C. The use of probe molecules would have somewhat perturbed the membrane. Shchipunov and Drachev (11) investigated the irreversible electrical breakdown of BLM formed from GMO in *n*-decane. They observed an increase in the average membrane lifetime below 14°C compared to that above 20°C, compatible with a gel to liquid-crystalline transition. Finally, light scattering studies of a GMO monolayer at the air/water interface fully compressed at low temperature (52) show an abrupt decrease of surface pressure at 15.5°C ($\Delta T_{1/2} \sim 0.5$°C) with no perceptible change at other temperatures. As expected, the changes were larger than observed for BLM (53). Reanalysis of the data of this experiment suggests small changes in scattered intensity about 12.5°C.

The changes in membrane properties observed near the transition in the present work are summarized in Fig. 16. The effects which bear most closely upon the nature of the transition are those in membrane thickness and dielectric anisotropy/order parameter. The changes in h seem to be reliable both in form and in magnitude, whereas the change in $\epsilon_a S_0$, while well established in form, is not certain as to magnitude.

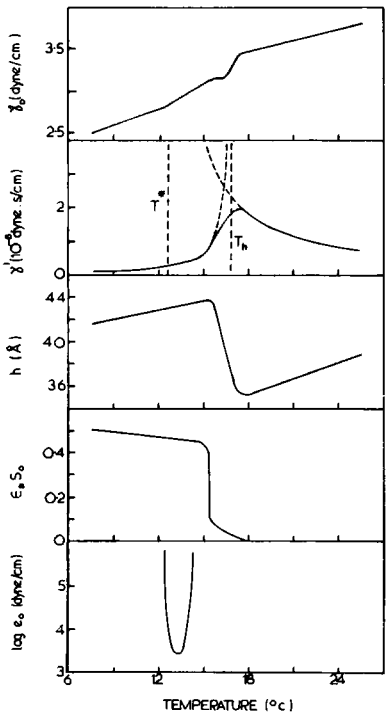

FIGURE 16 A schematic summary of the transitional changes in the various membrane properties probed.

The clearest indication that the observed transition at 16.6°C is accompanied by a change in the average conformational state of the lipid hydrocarbon chains is seen in *h*. Just below 16°C the BLM thickness is close to that expected for a bilayer of fully extended GMO molecules, falling at 16.6°C by 8Å. It has been suggested (9) that on average about seven *gauche* rotations occur per GMO molecule, changing the chain length by about 4.5Å, in good accord with the present result. The observed Δh accords well with theoretical predictions of chain-shortening in the melting of an all-*trans* hydrocarbon chain (44).

The behavior of $\epsilon_a S_0$ close to T_t affords further support for a chain-melting transition, being compatible with the limited available evidence. S_0 is known to change from close to 1.0 (ordered phase) to about 0.7 (fluid phase) in phospholipids (47). We assume similar changes would occur for chain-melting of GMO. There is little direct evidence concerning dielectric anisotropy in BLM. Above T_t ϵ_a/ϵ_m ~0.06 for GMO bilayers (42). Depolarized light scattering from phospholipid vesicles (54) suggest a substantial increase in ϵ_a below the transition. The analysis is somewhat uncertain, but a value of $\epsilon_a/\epsilon_m \sim 0.2$ below the transition (cf reference 22) seems reasonable. We thus infer that $\epsilon_a S_0$ should change substantially at the lipid transition. The *form* of the temperature variation of $\epsilon_a S_0$ is entirely compatible with a chain-melting transition.

We have associated a relaxation time τ ($= \gamma'/\gamma_0$) with the transverse membrane fluctuations governed by the elastic modulus γ: for 'solvent-free' BLM this was rather similar in both magnitude and cooperativity to the time scale for the appearance of *gauche* conformations in phospholipid membranes (38). The domination of capillary waves by a time-scale characteristic of lipid chain-melting further supports this interpretation of the transition at 16.6°C in GMO.

The transition temperature found for GMO, 16.6°C, is higher than expected for a chain-melting transition in a C_{18} lipid molecule with a *cis* double bond at the 9–10 position (see reference 55). Other effects should be considered. For example, changes in intra-molecular motions, detectable by Raman or infrared spectroscopy, have been observed in some membranes without accompanying thermally observable transition (56). However, the relevant intra-molecular motions are of high frequency and low amplitude and seem unlikely to strongly influence the comparatively low frequency disturbances observed in the present study. Further, such high frequency motions would not be liable to change the equilibrium order parameter, the molecular anisotropy or the lipid chain length. Changes in Raman-detectable motions are known to accompany a chain-melting transition but seem unlikely to simulate the effects of such a transition.

Certain other studies seem to confirm the association of the observed transition in GMO with considerable changes in the oleate chain. Over the range 12 to 17°C various

properties of a solution of oleic acid in CCl_4 showed marked changes in temperature dependence (61). The main effects occurred close to 17°C. The correspondence with the present GMO transition is clear. The rate of formation of bimolecular films of diolein shows a transitional change between 13 and 19°C, again apparently deriving from the presence of the oleate chain (57).

It now seems well established that GMO undergoes a transition in the region 12–17°C. Various membrane observables show transitional changes at rather different temperatures within this range. All of the results reported are explicable in terms of a chain-melting transition. Certain of the present observations seem to *demand* such an explanation.

Transition-associated Changes

The transition as observed in GMO/squalane membranes is summarized in Fig. 16. The form of the transitional changes in the various properties seems well established, but in some cases (already noted) the absolute magnitudes are uncertain. The effects occur over a restricted temperature range (12.5 to 17.5°C), several at common temperatures, perhaps indicating interconnections between the relevant properties.

On heating from below T_t, the first changes (~12.5°C) are an increase in the temperature gradient of tension (γ_0), the appearance of an observable transverse shear viscosity (γ') and the sudden decrease of the lateral compression modulus (e_0). Above 12.5°C the membrane viscosity increases as $(T_h - T)^{-1}$, T_h being 16.8°C. On further heating, e_0 increases at about 14°C, a temperature not associated with any other observed changes. About 15.7°C the transitional increase in γ_0 commences, γ' departs from its systematic increase, h starts to drop and $\epsilon_a S_0$ decreases discontinuously. This drop in $\epsilon_a S_0$ thus coincides with the apparent onset of the melting of the lipid acyl chains. Finally at ~17.3°C the transitional effects in both γ_0 and h cease and γ' starts to decrease as $(T - T^*)^{-1}$, T^* being 12.7°C. The transitional changes in γ_0, γ' and h all center upon T_t (= 16.6°C), γ_0 and h showing similar variations (sharp and symmetrical) around that temperature.

The variations of γ_0 and h over the whole temperature range covered (Figs. 6 and 10) are less similar than the changes close to T_t. The differences far from T_t suggest that these properties derive from rather different aspects of the membrane. The variations of both γ_0 and h at T_t reflect the chain-melting transition: h directly as hydrocarbon chain-length and γ_0 as average lipid packing density. The changes in $d\gamma_0/dT$ at 12.5 and 17°C arise from changes in interfacial entropy, via the Gibbs' adsorption isotherm. The positive dh^2/dT observed away from T_t derive from changes in inter-molecular interactions within and between the monolayers comprising the BLM.

It appears that the transition extends over a range of temperatures and that the various membrane properties observed reflect different aspects of the transition. Such behavior would be typical of a weak transition with strong pretransitional effects. Close to the transition, fluctuations appear easily in the membrane, involving small expenditure of energy. These fluctuations would affect different membrane properties in different ways.

The fluctuations evident in γ' suggest that the modulus γ (= $\gamma_0 - i\omega\gamma'$) reflects aspects of the membrane that are affected by the proximity of a critical point, whereas the h data suggest a rather clear first-order transition. Analysis of the fluctuations in γ' suggests that the critical temperature (T^*), at 12.7°C, is indeed close to the observed transition at 16.6°C. Similar fluctuations in membrane properties have been analyzed in such terms by Jahnig (36) for various systems and by Doniach (37) for the specific case of ionic permeability of lecithin bilayers. Recently the critical parameters of DPPC membranes have been determined (58): T^* at 38.2°C was rather below the transition at 41°C. The extent of the present pretransitional fluctuations (T^* to T_h, 12.7 to 16.8°C) may be seen as indicating the range of metastability in the temperature variation of the order parameter describing the lipid system (36).

The changes in membrane properties observed in the present work tend to cluster at two temperatures (about T^* and T_t). While the chain-melting might prohibit any true two-dimensional effects in amphiphilic systems, experiments on single bilayers are not affected by interbilayer forces that may enforce ordering in the third dimension of multi-lamellar systems (see 59 and the ensuing discussion). The present technique, applicable to single BLM and involving no molecular or macroscopic perturbation of the membrane, appears ideally suited to further study of the dimensionality of these transitions.

The transition in solvent-free membranes is quite sharp ($\Delta T_{1/2} \sim 1.5$°C). This is characteristic of transitions in pure lipid systems and confirms both that solvent is excluded from GMO/squalane membranes and that the GMO sample was rather pure. For GMO/decane membranes the transitional changes were of lower magnitude and were spread over a wider temperature range, showing the effects of the incorporated solvent upon the transition. The membrane viscosity might plausibly have had a rather small but nonzero value above ~16°C, but this is not proven.

Similar differences were found between MM and MR membranes of GMO by Fahey and Webb (10), who found greater lateral diffusion coefficients of molecular probes in the MR case than for MM. This parallels the different γ' values found here: substantially greater for solvent-free BLM than in the GMO/decane case.

CONCLUSIONS

Dynamic light scattering from membrane vibrations has been shown to be a sensitive spectroscopic tool for the investigation of phase transitions in both solvent and 'solvent-free' bilayer lipid membranes. In favorable cases (e.g. solvent-free BLM) the extraction of intensities from

heterodyne correlation functions has provided complementary information.

Many methods of probing membrane properties either sample rather vaguely defined properties (e.g. membrane fluidity) or are applicable only to multilamellar systems. In contrast, light scattering measures precisely defined membrane properties, including specific elastic moduli or viscosities, of *single* planar bilayers. Measurement of well-defined quantities is essential if these properties are to be related to inter- and intra-molecular processes.

Much of this paper has been concerned with data observed from one solvent-free BLM. This data was of particularly high quality (due to membrane stability and quality), justifying detailed analysis. While the results are substantiated by data from similar BLM, no one of these provided data of comparable quality. In such favorable cases the basic light scattering experiment provides information about a multiplicity of membrane properties simultaneously. Each concerns a different aspect of the transition and the consistency of the changes observed in all of them enables a coherent picture of the transition to be built up. This permits the accurate specification of the transition characteristics.

This study of solvent-free BLM formed from GMO dispersed in squalane yielded, for the first time, reliable data on the transitional changes in several properties of single bilayers. The main transition occurred at T_t = 16.6°C, in a temperature region where previous studies had suggested that GMO showed a transition. The present observations suggest a two-stage transition. Unlike the results of these earlier studies, the presently observed changes in membrane properties were such as to permit identification of the transition as a lipid chain-melting event. This is one of the major conclusions of our study. Other specific conclusions are:

(*a*) The membrane tension displays a two-stage change within the transitional region. A more rapid variation about T_t is superposed upon these slower changes.

(*b*) Pretransitional fluctuations in the transverse shear membrane viscosity suggest that the membrane at the transition is close to a critical point (T^* = 12.7°C).

(*c*) The capillary waves upon BLM display a relaxation time similar to those associated with chain-melting in phospholipids.

(*d*) The membrane thickness changes sharply at T_t by an amount consistent with a chain-melting transition ($\Delta T_{1/2}$ = 1.5°C).

(*e*) The membrane thickness shows a positive temperature gradient away from T_t. This result for a single BLM contrasts with negative gradients inferred from studies of multilamellar systems. The single bilayer result may arise from the effect of thickness fluctuations upon the mean value.

(*f*) The combination of dielectric anisotropy and molecular orientational order ($\epsilon_a S_0$) shows a discontinuous change at the onset ($T < T_t$) of the chain-melting event.

(*g*) The lateral compression modulus of the membrane shows a sharp minimum at temperatures rather below T_t, though close to the lower temperature change in tension and to T^*.

The studies of GMO membranes incorporating solvent in the bilayer structure demonstrated the effects of such solvent in broadening and reducing the transitional change. These observations emphasized the desirability of studying phase transitions without such additives.

Further experiments could reduce many of the uncertainties of the present results. Ambiguities in the analyses leading to $\epsilon_a S_0$ and to e_0 could be eliminated by suitable studies of depolarized scattering and of the spectrum of light scattered by compression waves respectively. The latter experiment would potentially yield information upon the dynamics of the events at the onset of the transition. Extensions of the present study to higher and lower temperatures would reveal how the observed pretransitional changes (e.g. in γ_0, γ' and h) carry over into more regular temperature variations. Studies of solvent-free BLM throughout complete cooling/heating cycles would be useful.

The potential of the present data on solvent-free membranes has not been exhausted by the analyses presented here. For example, if reliable data were available for molecular areas as a function of temperature a detailed study of the observed variation of membrane tension in terms of inter-molecular forces would become possible.

Dr. J. F. Crilly is thanked for communication of results before publication.

This work was supported by the United Kingdom Science and Engineering Research Council. GEC wishes to acknowledge financial support from the Department of Education for Northern Ireland.

Received for publication 17 May 1985 and in final form 21 October 1985.

REFERENCES

1. Lee, A. G. 1977. Lipid phase transitions and phase diagrams. I. Lipid phase transitions. *Biochim. Biophys. Acta.* 472:237–281.
2. Nelson, D. R., and B. I. Halperin. 1979. Dislocation-mediated melting in two dimensions. *Phys. Rev. B.* 19:2457–2484.
3. Milon, A., J. Ricka, S. -T. Sun, T. Tanaka, Y. Nakatani, and G. Durisson. 1984. Precise determination of the hydrodynamic radius of phospholipid vesicles near the phase transition. *Biochim. Biophys. Acta.* 777:331–333.
4. Lis, L. J., M. McAlister, N. Fuller, R. P. Rand, and V. A. Parsegian. 1982. Interactions between neutral phospholipid bilayer membranes. *Biophys. J.* 37:657–666.
5. Crilly, J. F., and J. C. Earnshaw. 1983. Photon correlation spectroscopy of bilayer lipid membranes. *Biophys. J.* 41:197–210.
6. Azzi, A. 1975. The application of fluorescent probes in membrane studies. *Q. Rev. Biophys.* 8:237–316.
7. Kwok, R., and E. Evans. 1981. Thermoelasticity of large lecithin bilayer vesicles. *Biophys. J.* 35:637–652.
8. Pagano, R. E., R. J. Cherry, and D. Chapman. 1973. Phase transitions and heterogeneity in lipid bilayers. *Science (Wash. DC).* 181:557–559.
9. White, S. H. 1975. Phase transitions in planar bilayer membranes. *Biophys. J.* 15:95–117.

10. Fahey, P. F., and W. W. Webb. 1978. Lateral diffusion in phospholipid bilayer membranes and multilamellar liquid crystals. *Biochemistry.* 17:3046–3053.
11. Shchipunov, Yu. A., and G. Yu. Drachev. 1982. An investigation of electrical breakdown of bimolecular lipid membranes. *Biochim. Biophys. Acta.* 691:353–358.
12. Crawford, G. E., and J. C. Earnshaw. 1984. Photon correlation spectroscopy as a probe of planar lipid bilayer phase transitions. *Europ. Biophys.* J. 11:25–33.
13. Goodrich, F. C. 1962. On the damping of water waves by monomolecular films *J. Phys. Chem.* 66:1858–1863.
14. Birecki, H., and N. M. Amer. 1979. Laser-ripplon scattering from lecithin monolayers at the air-water interface. *J. de Phys.* 40:C3-433–437.
15. Goodrich, F. C. 1961. The mathematical theory of capillarity. II. *Proc. R. Soc. Lond. A.* 260:490–502.
16. Kramer, L. 1971. Theory of light scattering from fluctuations of membranes and monolayers. *J. Chem. Phys.* 55:2097–2105.
17. Hladky, S. B., and D. W. R. Gruen. 1982. Thickness fluctuations in black lipid membranes. *Biophys. J.* 38:251–258.
18. Vrij, A. 1968. Light scattering from liquid interfaces. *Adv. Coll. Interf. Sci.* 2:39–64.
19. Bouchiat, M. A., and D. Langevin. 1978. Relation between molecular properties and the intensity scattered by a liquid interface. *J. Coll. Interf. Sci.* 63:193–211.
20. Crilly, J. F. 1981. Photon correlation spectroscopy of planar bilayer lipid membranes. Ph.D. thesis, Queen's University of Belfast. 372 pp.
21. Herpin, J. C., and J. Meunier. 1974. Etude spectrale de la lumière diffusée par les fluctuations thermiques de l'interface liquide vapeur de CO_2 près de son point critique. Mesure de la tension superficielle et de la viscosité. *J. de Phys.* 35:847–859.
22. Fan, C. 1973. Fluctuations and light scattering from anisotropic interfaces. *J. Coll. Interf. Sci.* 44:369–381.
23. de Gennes, P. G. 1974. The Physics of Liquid Crystals. Oxford University Press, Oxford. 333 pp.
24. Murray, E. C., and R. N. Keller. 1969. Purification of hydrocarbon solvents with a silver nitrate column. *J. Organic Chem.* 34:2234–2235.
25. Crilly, J. F., and J. C. Earnshaw. 1985. Light scattering from fluid interfaces: considerations of some instrumental effects. *J. Phys. D.* 18:609–616.
26. Crawford, G. E. 1984. Phase transitions in monoglyceride bilayer membranes. Ph.D. thesis, Queen's University of Belfast. 236 pp.
27. Crawford, G. E., and J. C. Earnshaw. 1985. Light scattering by lipid bilayers: intensity determination by heterodyne correlation. *J. Phys. D.* 18:1029–1035.
28. International Critical Tables. 1928. National Research Council. 5:12–19.
29. Requena, J., and D. A. Haydon. 1975. Van der Waals forces in oil-water systems from the study of thin lipid films. II The dependence of the van der Waals free energy of thinning on film composition and structure. *Proc. R. Soc. Lond. A.* 347:161–177.
30. Tien, H. Ti. 1974. Bilayer lipid membranes (BLM) theory and practice. Marcel Dekker, New York. 655 pp.
31. Lutton, E. S., C. E. Stauffer, J. B. Martin, and A. J. Fehl. 1969. Solid and liquid monomolecular films at oil/H_2O interfaces. *J. Coll. Interf. Sci.* 30:283–290.
32. Pagano, R. E., J. M. Ruysschaert, and I. R. Miller. 1972. The molecular composition of some lipid bilayer membranes in aqueous solution. *J. Membr. Biol.* 10:11–30.
33. White, S. H. 1977. Studies of the physical chemistry of planar bilayer membranes using high-precision measurements of specific capacitance. *Ann. NY Acad. Sci.* 303:243–265.
34. Moore, W. J., and H. Eyring. 1938. Theory of the viscosity of unimolecular films. *J. Chem. Phys.* 6:391–394.
35. Jahnig, F. 1981. Critical effects from lipid-protein interaction in membranes. I. Theoretical description. *Biophys. J.* 36:329–345.
36. Jahnig, F. 1981. Critical effects from lipid-protein interaction in membranes. II. Interpretation of experimental results. *Biophys. J.* 36:347–357.
37. Doniach, S. 1978. Thermodynamic fluctuations in phospholipid bilayers. *J. Chem. Phys.* 68:4912–4916.
38. Holzwarth, J. F., V. Eck, and A. Genz. 1984. Iodine laser temperature jump from picoseconds to seconds: relaxation processes of phospholipid bilayers. *In* Spectroscopy and dynamics of biological systems. P. M. Bailey and R. Dale, editors. Academic Press, Ltd., London. 351–377.
39. Eck, V., and J. F. Holzwarth. 1983. Fast dynamic phenomena in vesicles of phospholipids during phase transitions. Proceedings of the International Symposium on surfactants in solution. K. L. Mittal, editor. Plenum Publishing Corp., New York. 3:2059–2080.
40. Cherry, R. J., and D. Chapman. 1969. Optical properties of black lecithin films. *J. Mol. Biol.* 40:19–32.
41. Stamatoff, J., B. Feuer, H. J. Guggenheim, G. Tellez, and T. Yamane. 1982. Amplitude of rippling in the P_β phase of dipalmitoylphosphatidylcholine bilayers. *Biophys. J.* 38:217–226.
42. Dilger, J. P. 1981. The thickness of monoolein lipid bilayers as determined from reflectance measurements. *Biochim. Biophys. Acta.* 645:357–363.
43. Trauble, H., H. Eibl, and H. Sawada. 1974. Respiration—a critical phenomenon? Lipid phase transitions in the lung alveolar surfactant. *Naturwissenschaften.* 61:344–354.
44. Kambara, T., and N. Sasaki. 1984. A self-consistent chain model for the phase transitions in lipid bilayer membranes. *Biophys. J.* 46:371–382.
45. Seelig, A., and J. Seelig. 1974. The dynamic structure of fatty acyl chains in a phospholipid bilayer measured by deuterium magnetic resonance. *Biochemistry.* 13:4839–4845.
46. Wallach, D. F. H., and R. J. Winzler. 1974. Evolving strategies and tactics in membrane research. Springer-Verlag, Berlin. 381 pp.
47. Seelig, J., and W. Neiderberger. 1974. Two pictures of a lipid bilayer. A comparison between deuterium label and spin-label experiments. *Biochemistry.* 13:1585–1588.
48. Handbook of Chemistry and Physics, 55th ed. 1974. Chemical Rubber Publishing Co., Cleveland.
49. Nagle, J. F., and H. L. Scott. 1978. Lateral compressibility of lipid mono- and bilayers. Theory of membrane permeability. *Biochim. Biophys. Acta.* 513:236–243.
50. Marcelja, S., and J. Wolfe. 1979. Properties of bilayer membranes in the phase transition or phase separation region. *Biochim. Biophys. Acta.* 557:24–31.
51. Lis, L. J., M. McAlister, N. Fuller, R. P. Rand, and V. A. Parsegian. 1982. Measurement of the lateral compressibility of several phospholipid bilayers. *Biophys. J.* 37:667–672.
52. Crilly, J. F., and J. C. Earnshaw. 1983. Photon correlation studies of phase transitions in lipid monolayers. The application of laser light scattering to the study of biological motion. J. C. Earnshaw and M. W. Steer, editors. Plenum Publishing Corp. New York. 325–331.
53. Albon, N., and J. F. Baret. 1983. Comparisons and correlations between the properties of lipid molecules in crystals, bilayer dispersions in water, and monolayers on a water surface. *J. Coll. Interf. Sci.* 92:545–560.
54. Mishima, K. 1981. Depolarized light-scattering studies of bilayer structures in phospholipid vesicles. *Biochim. Biophys. Acta.* 648:162–168.
55. Barton, P. G., and F. D. Gunstone. 1975. Hydrocarbon chain packing and molecular motion in phospholipid bilayers formed from unsaturated lecithins. *J. Biol. Chem.* 250:4470–4476.

56. Wallach, D. F. H., S. P. Verma, and J. Fookson. 1979. Application of laser Raman and infrared spectroscopy to the analysis of membrane structure. *Biochim. Biophys. Acta.* 559:153–208.
57. Seccia, F., A. G. Bois, L. Casalta, and J. F. Baret. 1979. The formation rate of diolein bimolecular lipid membranes. *Coll. Poly. Sci.* 257:539–545.
58. Sugar, I. P., and T. E. Thompson. 1985. Effects of thermodynamic fields on the phase transition properties and stability of phospholipid bilayers: Landau theory of one-component systems. *Biophys. J.* 47:(2, Pt. 2):246*a*. (Abstr.)
59. Doniach, S. 1980. Melting in phospholipids and in smectics—a comparison. Ordering in two dimensions. S. K. Sinha, editor. Elsevier North-Holland, New York. 67–72.
60. Evans, E., and R. Kwok. 1982. Mechanical Calorimetry of Large Dimyristoylphosphatidylcholine Vesicles in the Phase Transition Region. *Biochemistry.* 21:4874–4879.
61. Champion, J. V., J. F. Crilly, and R. P. Fatom. Evidence for a Thermotropic Phase Transition in Oleic Acid. *J. Chem. Soc. Farad. Trans. II.* In press.
62. Jakeman, E. 1974. Photon Correlation. Photon Correlation and Light Beating Spectroscopy. H. Z. Cummins and E. R. Pike, editors. Plenum Publishing Corp., New York. 75–149.